N88-16659

RECENT SIKORSKY R&D PROGRESS

Abstract

This paper summarizes the recent activities and progress in four specific areas of Sikorsky's independent research and development program. No attempt is made to cover the full spectrum of R&D activities. In fact, even some major thrusts over the past few years are not covered. Since the beginning of the S-76 design in 1974, Sikorsky has been aggressively developing the technology for using composite materials in helicopter design. This effort included ACAP, of course, but has gone beyond that now to concepts as those incorporated by Sikorsky in the Piaggio P-188.

Four specific topics are covered here: advanced cockpit/ controller efforts, fly-by-wire controls on RSRA/X-Wing, vibration control via higher harmonic control, and main rotor aerodynamic improvements.

Sikorsky Helicopter Advanced Demonstration of Operational Workload (SHADOW) aircraft successfully flew structural flights in 1985. An electronic Fly-By-Wire flight control was incorporated and the evaluation pilot avionics that permit single pilot operation were installed. Single piloted flight test of the SHADOW aircraft began in 1986. This flying test bed is being used to evaluate various configuration of CRT displays, sidearm controllers and voice interactive systems as proposed candidates for the U.S. Army family light helicopters designated LHX.

Sikorsky has full authority fly-by-wire flight-critical control system in test for RSRA/X-Wing. The multi-processor quad-redundant flight control computer system has undergone successful initial testing in a laboratory installation. This computer complex is believed to be, with the exception of the space shuttle, the most sophisticated flight critical system in existence today. The software associated with this application controls essentially all aspects of the vehicle's mechanisms. This software is now undergoing extensive verification and validation. In the process of this software confirmation the complete vehicle management system is being exercised in the specially developed X-Wing Vehicle Management Systems Laboratory.

C-4

Sikorsky's full authority fly-by-wire flight control systems has been aided by the IR&D supported development of the redundancy management methodology and an automated software verification methodology. Redundancy management methodology was formulated and utilized to establish a systematic approach for the development of the X-Wing flight-critical control system design. Also evolved was a library of preferred software and hardware approaches to implement those redudancy concepts. The automated software verification has been based on obtaining identical output responses from dissimilarly programmed test software and from actual flight system software when both are subjected to a common input. As changes are made to the program, both sets of software are modified and are exercised automatically with thousands of preselected control input combinations through a computerized procedure resident on a host computer.

A flight test of open-loop higher harmonic control has been conducted on the S-76 aircraft. This project extended the envelope of HHC experimental flight test investigation to gross weights of approximately 10,000 lbs. and 150 knots forward speed. A 1.5-hour ground test and 23-hour flight test provided a demonstration of the effectiveness of HHC in the control of vibration, replacing the conventional rotor head and airframe absorbers.

Substantial vibration reduction was achieved by applying preset amplitudes and phases of HHC through the main flight controls servos. Test conditions showed vibration reduction through a series of maneuvers as well as in level flight. The objective of providing a body of engineering data on the effects and requirements of HHC was also met. Measurements were made of the effects of HHC on loads, stresses, aerodynamic performance and acoustics. The HHC servo motion amplitude and hydraulic flow requirements to control vibration at high speed were also determined. These data are invaluable to support extrapolation of HHC applications to new aircraft such as the LHX.

Rotor performance has been upgraded through both refined geometry and improved airfoils. To minimize the unfavorable performance and noise effects of blade tip vortices in proximity to the top of the following blade, blades were modified to incorporate anhedral (droop) on the blade tips. Model and full scale hover tests showed significant performance benefits, and analysis predicted no adverse effects in forward flight. Flight tests were then conducted which verified that and provided useful blade loads data.

A third-generation high life airfoil, the SC2110, was developed as a replacement for the SC1094R8. This airfoil section was designed to retain the high maximum lift capability of the earlier section but possess significantly reduced drag at high Mach numbers and a higher drag divergence Mach number. It is significant that the

entire design process was carried out analytically using 2-dimensional computational fluid dynamic methodology. Subsequent wind tunnel testing of the optimized design fully validated the predicted results. The new airfoil design, while retaining the excellent C_{LMAX} characteristics of the BLACK HAWK high life section, has transonic drag levels no greater than the BLACK HAWK outboard section. This represents a very large improvement in airfoil technology.

SIKORSKY HELICOPTER ADVANCED DEMONSTRATION OF OPERATIONAL WORKLOAD (SHADOW)

SHADOW is an experimental helicopter, based on an S-76A, that is exploring the functional, automation and integration requirements necessary for single pilot operation of future military rotorcraft. This paper describes the physical aircraft, its flight controls and the avionics that supported the ARTI flight test experiments including visibility tests.

Aircraft Description

The physical layout of the crew and equipment will be described starting with the forward portion of SHADOW and working aft. The host aircraft is a standard Sikorsky S-76A with the nose-located electronics bay removed and an excellent visibility, single pilot cockpit attached by the means of longerons extended from the original aircraft (Fig. 1). The Evaluation Pilot for a total crew of five (Fig. 2). In the main cabin, there is a a Safety Pilot (in the conventional location) with mechanical flight controls and standard S-76A instruments, an Evaluation Copilot beside him with electronic flight controls, and two Flight Engineers in the passenger cabin area (EP) sits up in the EP cockpit has full aircraft status and control with the exception of engine and landing gear control for safety reasons.

Using "glass" instrumentation in the EP cockpit (Fig. 3) permits extensive use of both traditional symbology as well more highly integrated icons to reduce pilot workload. A Honeywell monocular (part of IHADSS) Helmet Mounted Display (HMD) is the primary display medium. A Polhemus Navigation magnetic head tracker is used to determine head angles. There are two center console mounted Rockwell-Collins full color Head Down Displays (HDD) called the Tactical Situation Display (TSD) and System Management Display (SMD). There is a bezel assembly made by Photoetch with 24 switches, 6 on a side, for each HDD. There are 5 Honeywell Programmable Display Pushbuttons (PDP's) on either side of the TSD. A Dorman-Bogdonoff touchscreen is on each of the HDD's. A Shure microphone is used for both standard ICS and the Hamilton-Standard Voice Interactive System (VIS). The VIS is actuated by a two position rocker switch located on the right-hand flight control grip. The Northrop 8-12 micron FLIR turret is mounted at the extreme forward portion of the fuselage. A standard SH-60 Seahawk seat is used. There are miscellaneous control and test panels and the ICS panel located on either side of the seat.

The FBW system uses Measurement Systems dual-redundant, strain gauge type, limited motion flight control transducers. The grips are a Sikorsky custom design made by Bendix. A Sikorsky "slide" type control can be used in place of the left side flight control. The foot pedals, for optional yaw control (2+1+1 configuration),

are either force or limited motion type. Pilot and cockpit avionic cooling is provided by a Keith air conditioning system.

Figure 4, SHADOW avionic layout, shows the placement of the various boxes. Individual box location was carefully chosen to eliminate the need for ballast to establish proper center of gravity (CG).

ARTI - Flight Test

The flight test objectives were to investigate design questions which could not be adequately dealt with in the ground-based simulator and to provide a real world anchor point for simulation results. The first step was development of a flight control system that was both safe and a reasonable approximation of LHX pilot workload. The aircraft was then utilized to investigate cockpit visibility HMD FOV and HMD symbology.

Flight Controls Tests

The purpose of the flight controls tests were to ensure the flight safety of the Sidearm Control System (SCS) and that pilot workload was sufficiently low to perform the other ARTI experiments. Tests of the SCS stability, shutdowns, overrides, stick sensitivities and SCS configurations (2+1+1, 3+1, and 4+0) were performed.

With the present Shadow-ARTI control laws, the pilots preferred to use the 3+1 configuration which included the right hand 3 axis sidearm controller for pitch, roll, and yaw control along with a left hand displacement collective stick. All the configurations shared deficiencies which were a function of using force instead of displacement controls. Increasing the compliance of the force controller as well as control law improvement may help to alleviate these problems. Inadvertent pitch and roll rates during takeoff and landing were noted. Improved logic to fade in/out stabilization during these maneuvers should help to solve this problem.

The workload of the Shadow-ARTI flight control system, although reasonable for the initial ARTI studies, was still too high to perform NOE tasks. The additions of altitude stabilization, altitude hold and heading hold should lower pilot workload enough to perform NOE tasks. These features are included in the Sikorsky

Model Following Control Laws which are in shakedown flight testing.

Cockpit Visibility Test

The exterior cockpit vision requirement is an issue with major impact on the design of the ARTI/LHX cockpit. LHX concepts have ranged from "windowless" to versions which maximize the glass area. Between these extremes are questions which relate to the size and shape of consoles and their associated glareshield, the need for chin windows and the masking of overhead windows by roof-mounted EOTADS (Electro-Optical Targeting and Designation System) units. These studies used the basic Shadow as a baseline for the evaluation of likely cockpit design features. Three experimental configurations were evaluated The first configuration represents a two CRT design with the displays arranged vertically. The second configuration was also a two CRT design but with the displays arranged horizontally. The third was a horizontal arrangement of three CRTs. Each of these has advantages and disadvantages in terms of functionality and cockpit geometry but the purpose of this study was to look at their effect on external vision while flying a variety of tasks which sample the critical elements of the LHX mission. Each of these had no chin windows because of crew armor protection. In addition, all had no overhead windows to simulate the EOTADS position.

Three Sikorsky pilots tested all the configurations and were asked to perform the same maneuvers for each. These included hovering, hover turns, a bob-up, a figure-eight and sideward flight at low speed, cruise flight at 2000 ft., and two different landings. These maneuvers required the pilot to use several areas of external visibility: over-the-nose, forward-low, down, side and overhead. All tests were conducted with the integrated helmet and display sighting system (IHADSS) with symbology from the on-board Gaertner display generator. The Polhemus head tracker provided data to the display generator on the pilot's head position in azimuth, elevation and roll. The position data from the head tracker was recorded on a strip chart recorder in the aircraft along with aircraft attitude, altitude, and airspeed. During all maneuvers, over-the-shoulder video with a voice track was recorded. At the conclusion of the flight each pilot was given a form for comment on the configurations tested and an overall rating. The rating system was based on the traditional Cooper-Harper rating scale, with the wording modified for this investigation.

Pilots comments indicated several critical areas of visibility. In the hovering tasks, 30 to 45 degrees of azimuth on either side of the console was the primary area for forward-low reference with the chin windows giving peripheral cues to aid in position and altitude control. There was degradation in performance in hover for lateral station keeping with the loss of chin windows and

continuing loss of performance with larger consoles. The loss of visibility forward-low was also evident in increased time when executing an approach to land.

The precision of hover and hover turns is clearly affected adversely by cockpit configurations that have diminished exterior vision. Pilots compensate for the lack of vision by increasing the amplitude and frequency of their head motion. This adds to cockpit workload and is reflected in the pilot ratings of the configuration. Pilot comments point out the importance of the overhead and chin windows. The overall conclusion from this study is an understanding of how the tradeoffs between external visibility and other design parameters can significantly impact both pilot performance and workload.

HMD FOV Test

The field of view of a helmet-mounted display has been identified as a major driver of technical risk for the single pilot LHX. The purpose of this study is to assess the effects of field of view on flight performance. It is recognized that there are several HM design parameters which impact pilot performance, i.e., resolution brightness, etc, besides FOV. Due to experimental limitations, we confined our investigation to field of view alone. Three configuration were compared with a baseline which consisted of the IHADSS display unit mounted on a standard IHADSS helmet. Thus, with the baseline the symbology was presented in a 30° x 40° area, but the FOV was only restricted by the helmet itself.

To modify the helmet field of view, three masks were created which could be taped directly to the pilot's helmet. These masks restricted the field of view to 30 x 40, 40 x 80 and 60 x 120 degrees of azimuth and elevation respectively.

The procedures and format of the investigation were identical to the cockpit visibility experiment. Three Sikorsky pilots tested all the configurations and performed the same manuevers. The tests were conducted with symbology presented on the IHADSS.

Similar to the cockpit visibility experiment, the data indicated a trend of decreasing pilot performance as the field-of-view was reduced. This could be seen in comparisons of pilot performance, the frequency of head motion in the cockpit, and the pilot comments. The accuracy of the hovering tasks were those most affected by the restricted field of view.

There is a strong overall relationship between performance precision and HMD field of view. In addition, an increase in pilot effort to compensate for FOV restriction is clearly evident in the head motion data for tasks involving anything but straight ahead vision. The results of these tests will facilitate the LHX HMD development.

HMD Symbology

The Shadow HMD symbology was virtually identical to that used in the simulation. Evaluation of this symbology, for the most part, was done in the fixed-base simulation. However, several aspects of the symbol set could only be properly evaluated in actual flight. Additionally, the flight tests validated the simulator fidelity.

In general, the concept of "contact analog" symbology, where the symbology overload and supplemented cues from the outside visual world, worked very well in flight. The cues were very natural because of the close correspondence to contact flight cues. Pilots using the cues for the first time had no difficulty interpreting the display and no control reversals were observed.

Summary

In summary, the ARTI Task VI Flight program has proven SHADOW to be a flexible, "flying" simulation. The close correspondence of its cockpit and symbology with the ground-based simulator have provided an excellent mix of capabilities. This similarity have helps to anchor the simulation results to the real world. by alternately flying SHADOW and the ground-based simulator, the program pilots are very aware of simulation strengths and weaknesses.

Several important single pilot issues have been considered. The aircraft has provided the truly unique opportunity to investigate cockpit visibility in flight at a time when the LHX design can be modified. This study has shown the sensitivity of visual workload and performance precision to cockpit configuration. The HMD field of view study clearly confirms the need for a wide field of view helmet display system.

X-WING/RSRA FLY-BY-WIRE VEHICLE CONTROL SYSTEM

The RSRA/X-Wing program mates a circulation control rotor with the NASA Rotor Systems Research Aircraft (RSRA) for the prime objective of demonstrating an inflight conversion to a stopped rotor state, a unique capability of the X-Wing rotor (Fig. 6). The control system of such a vehicle faces significant challenges. It must first be designed to accommodate the equivalent of three vehicles since the X-Wing operates in a rotary wing mode, a fixed wing mode, and in the interim conversion state. It must achieve rotor cyclic control via a pneumatic medium. It is a full authority fly-by-wire system for all functions, except the existing aileron, rudder and elevator controls which are retained from the RSRA, and provides a mechanical override capability for the safety pilot. For the evaluation on the RSRA it must provide control sharing in recognition of an 20,000+ pound rotor capability mated with a 30,000 plus pound vehicle. Furthermore the control system rapidly evolves into a Vehicle Management System (VMS) controlling many subsystems and providing functions beyond the classical flight control system-this driven both by prudent, efficient design and by redundancy requirements of allied subsystems.

A review of the X-Wing plant identifies the major functions required of the VMS (Fig. 7):

- Control of the circulation control rotor
- Main rotor blade collective pitch control
- Automatic conversion control
- Pneumatic system control
- Air data computation
- Vibration alleviation via Higher Harmonic Control (HHC)

The control approach defined to meet those challenges includes the elements of: an integrated Vehicle Management System, full redundancy treatment for the X-Wing control portions, use of the RSRA both as a safety backup and for control sharing and a digital fly-by-wire approach. A design goal was to be transferable as a stand alone system to a pure X-Wing vehicle.

Major subsystems are the pneumatic, rotor conversion, HHC and the mechanical collective. The pheumatic control includes compressor control via Inlet Guide Vane (IGV) positioning to provide required plenum pressure, modulating discharge valves to avoid compressor stall and the pneumatic control valve actuators to establish the airflow to each blade's leading and trailing edges. The conversion subsystem controls both the steady states (rotary and stopped) of the rotor via locking actuators and the conversion between those states via the clutch or the rotor brake/indexing functions for the rotary and stopped conversions respectively. Vibration alleviation is provided by the HHC system which is

implemented in two forms, a scheduled system resident in the flight critical portion of the VMS and a closed loop active HHC configured in a fail safe (dual) computer module. The mechanical collective pitch subsystem is a quad electrically controlled, dual hydraulic powered system providing a range of +10° operating against the very formidable loads of the rigid rotor.

System redundancy is predicated upon the design goals of two-fail operational for similar failures in flight critical systems and fail-safe for "mission" critical elements. The architectural implementation is basically quadruple electrical and dual hydraulic. Elements such as the computers, sensors, and electro-hydraulic servo valves are quadruple. In some areas equivalent redundancy has been achieved by structuring the system to avail the program of existing hardware or the unique features or a subsystem (Fig. 8,9). The clutch control system is an example of the former where dual Clutch Control Units (CCU) are supplemented by the quad flight control computers which provide independent monitoring, selection, and backup control. The PCV's illustrate the latter. Features such as twenty-four valves about the perimeter sampled two at a time by the blade receivers are supplemented by averaging springs to position a bypassed actuator at a position midway between its neighbors. The combination of these permit the PCV actuator to be configured with only dual electrical coil servo valves.

Software redundancy is addressed by the inclusion of Back-Up Control Software (BUCS) in recognition of the common mode software failure mode (Fig. 10). It treats the probability that error free software may not exist, in spite of extensive verification and validation, in a 120,000 line program. The BUCS design utilizes isolated, dissimilar software executed by the same quadruple computers. It is activated by either automatic transfer, when certain failure conditions are encountered, or pilot initiated transfer. Simplicity, which equates to high confidence in software quality when subjected to extensive validation, is the essence of the BUCS. Accordingly it is configured with a very simple control law adequate to affect a precautionary landing.

Major hardware elements of the system are the Flight Control Computer (FCC), the Actuator Control Module (ACM), and the Pneumatic Control Valve (PCV). The FCC is a Z8002 microprocessor - based computer with a very extensive input/output signal conditioning complement mandated by the multiplicity of system sensors and actuators. It's throughput capability exceeds two and a half million operations per second, achieved by virtue of a lattice matrix architecture which provides four microproccessors per channel in a parallel/co-processor configuration.

The complete computer ship set is comprised of four boxes (Fig. 11) all containing identical MFCS and BUCS (flight critical) functions. In addition, 2 of the boxes contain AFCS and the other two boxes contain an active HHC (Higher Harmonic Control).

The ACM is a standardized quadruple actuator interface between the FCC and the hydraulic ram which is sized for the load of the specific application. It exhibits hydologic, hydraulic shutdown interlock, and IBIT features. The PCV actuator is a hydraulic powered actuator controlled by either of two computers. Two actuators are housed in an assembly, one for the leading edge valve and one for the trailing edge valve control via concentric shafts.

The design phases are essentially complete and emphasis has shifted to development and test of the system and its target vehicle. These phases are structured to progressively evaluate the system at higher level of integration prior to committing to the ultimate objective of an inflight conversion. Addressed hereafter are the wind tunnel testing, Ames vertical Motion System evaluation, software verification, hardware airworthiness evaluation, integrated system validation, power system test bed survey, and flight demonstration (Fig. 12).

The wind tunnel testing is conducted with a one sixth aerodynamically scaled RSRA fuselage outfitted with a circulation control rotor and a pneumatic distribution system. Control of the rotor can be effected either manually from an operator's console or automatically from a SEL computer based implementation of the vehicle management system. The data generated by this testing, which explores the stopped rotor, conversion, and rotary wing envelopes, provides a data base to judge the adequacy of or update the models used to analyze the control system needs and to evaluate the efficacy of the implementation during the system validation testing.

Several entries into the Ames Vertical Motion Simulator provided an opportunity to evaluate the controllability of the air vehicle in its several modes of flight with the intended control laws modeled. The evaluation addressed the full-up control laws (MFCS), submodes of the MFCS for degraded operation (direct link and plenum dump), and the backup control software (BUCS) mode. This testing provided an early indication of the viability of these modes under various flights and landing conditions. A comparison of the simulator model when flown rotor off with the actual flight test observations on aircraft 740, formed the basis of the simulation model validation.

The software verification is conducted by Hamilton Standard (HSD) (the provider of the FCC and its software). It is a highly automated process subjecting the software to approximately 1400 test cases designed by a HSD systems engineering team (as differentiated from the software engineering team which designed the software) and monitored for total coverage of the SA requirements by SA digital system engineers (Fig. 13). The automation is provided by the HSD designed Systems Integration and Test Stand (SITS) which serves both as a software development and test facility (Fig. 14). The PDP11 based SITS includes actuator and sensor simulators, fault insertion means and brassboard (RAM) versions of the FCC. In addition an extensive library of software provides functions such as test case development, expected results comparison, and editing.

A special provision has been provided to address the flight control law (as opposed to executive, redundancy management and built-in-test) portion of the software. This area is deemed to be judged by the most subjective criteria and hence prone to the most revision and subsequent reverification. To expedite that process, an automated software verification system was developed and is in operation (Fig. 13). It is based on obtaining identical output responses from dissimilarly programmed test software and from actual flight system software when both are subjected to a common input. As changes are made to the program, both sets of software are modified (independently) and are then exercised automatically with a multiplicity of preselected control input combinations through a computerized procedure resident on a host computer.

The airworthiness evaluation of the flight control system hardware is a relatively conventional approach patterned from MIL-STD-810C. The FCC, for example, is subjected to high/low temperature operational evaluation, vibration resonance search and cycling, shock, humidity and EMI testing. All as a confirmation of design criteria and the effectiveness of features such as the heat transfer means and filter pin connectors. The flight critical nature of the components is further addressed by a broad application of "burn-in" conditioning during the fabrication/acceptance test process. For the FCC, this includes random vibration and ten thermal cycles, the last five of which must be failure free.

The most extensive and detailed testing applied to the VMS is the system integration and validation testing conducted in the Vehicle Management System Laboratory (VMSL) (Fig. 16). This is a hardware in the loop/real time simulation test of the entire control sysem as commanded by the software resident in the FCC's. The VMSL is a specially developed facility for the RSRA X-Wing providing for semi-automatic application of test conditions to the system under test.

Key elements of the VMSL are:

- A Sikorsky-based second SITS is the heart of the VMSL providing the semi-automated testing ability. It includes the capability to generate and store test cases and apply simulated faults via its sensor and actuator simulators.

- Dual SEL-9780's host the aerodynamic and pneumatic aircraft simulations. The simulation is a real time derivative of the master GENHEL model used for the handling qualities analysis and control system design.

- Brassboard (laboratory) FCC configured with RAM are included for early development work. Flightworthy (EPROM) units can be substituted individually, or as a set, to test flight hardware prior to usage.

- A fixed based cockpit with side by side seating representative of the RSRA is provided to permit pilot interaction evaluation for effects/response and procedures refinement. This is outfitted with a simple display to provide VFR flight tasks.

- A Ground Based Data System (GBDS) identical to those at the wind tunnel and flight test sites for data collection, storage, and processing. It includes a link between the three systems to share data bases and permits comparison between predictions and results.

- A full complement of sensors and actuators, including the 48 actuator PCV array and, with simulated loads, are included.

- Hydraulic and electrical supplies including the digital power switching units which provide the uninterrupted power for the FCC's.

The integration and validation testing is achieved by the application of an array of test cases to the system (Fig. 17). The program is structured to progressively qualify the system for PSTB, stopped rotor (SR) flight, rotary wing (RW) flight, and conversion flight. Two software programs are involved: The stopped rotor/direct link (SR/DL) package utilized for the first two phases (PSTB and SR) and the Unified Control Laws (UCL) used for the latter two phases (RW and conversion). The SR/DL is a simplified derivative of the UCL created to provide earlier availablity for flight. A estimated 5000 test cases are being created for validation. The PSTB release assumes 750 successful

tests; the SR flight 2080 including the 750 for the PSTB. The testing validates such features as redundancy management including reconfiguration, dynamic response, stability, compressor control, actuator management, built in test and BUCS.

The propulsion system Test Bed (PSTB) is a power train endurance test facility typical of those applied to most new aircraft programs. For the RSRA X-Wing its role has been expanded to be a part of the control system validation process. Several entries are intended, addressing the progressively increased functions provided by the VMS. The first entry precedes the stopped rotor blowing flight phase and focuses upon the pneumatic control and distribution system. The high power demand (2000 HP) and flows (29 lbs per second) preclude the inclusion of a real compressor in the VMSL, making its validation cases dependent on computer models.

The PSTB confirms not only the ability of the VMS to control the compressor but also the operation of the PCV system in the presence of flow. Specific emphasis is upon regulation of plenum pressure, response to demands, the effect of pneumatic lags, and the stall avoidance and recovery operation. Later tests address the hub moment force (HMF) sensing system, in terms of accuracy and cross axis effects, and the conversion system operating in the presence of actual inertias and loads but with the obvious exception of forward flight effects.

The culmination of all the testing is a successful in-flight conversion. The flight program is structured as a gradual buildup to that event (Fig. 18). First emphasis is upon the rotor-less RSRA flying as a fixed wing aircraft. This starts as a replication of the qualifying work done on RSRA #740 in 1984 and incrementing the gross weight and vertical center of gravity to the X-Wing design points. The X-Wing rotor is then installed first as a two bladed "Wing" and then in the four bladed X- both without circulation control activated. The next phase introduces the circulation control blowing while flying in the stopped rotor configuration. The VMS is operational with the stopped rotor/direct link software executed by the FCC to provide pneumatic subsystem control and flight control of both the CCR rotor and the fixed wing surfaces. The conversion system is mechanically "locked" into the stopped rotor configuration. The BUCS is also installed as a necessary safety feature for any flight test. The next two flight phases require the full operational VMS as represented by the Unified Control Law (UCL) software programs for the FCC. The rotary wing phase explores the other end condition of the conversion. The VMS provides the means to turn up the rotor during the ground starting procedure and then maintains the rotor coupled to the propulsion system via the clutch. Vehicle control during flight is effected via the VMS which also commands fixed wing surfaces to effect the necessary load sharing.

Also required during the rotary and conversion flight phases is the higher harmonic control system. The mandatory bounding of vibration is provided by the scheduled (as a function of airspeed, rotor RPM and load) HHC contained in the quadruple MFCS. This is supplemented by the dual active HHC whose commands are added to those of the scheduled HHC. The active HHC is responsive to observed vibrations and particulary addresses transients such a encountered due to maneuvering flight, gusts, or resonance crossing during conversion.

The conversion phase is also approached gradually by use of the conversion abort feature. A conversion can thereby be initiated, permitted to progress to a rotor RPM difference and then returned to the initial condition. This is possible starting from either end state with software safeguards included to preclude a "turnabout" at a resonant frequency point. The flight control provided by the VMS is as its name implies, a unified control using essentially the same control law structure for rotary, stopped and conversion control. Some gains are adjusted with rotor speed and the rate crossfeeds and controls crosscoupling germaine to the rotary mode are phased out.

Many features are included in the basic system to support system flight development. These include (Fig. 19):

- Ultraviolet erasable memory to permit program update without the risk of RAM
- Alternate gain selections by axis which switches in an alternate array of gains previously validated as safe thru VMSL testing.
- Test inputs to provide response measurement in all axes when the system is pertubated by pulse, sine, step or doublet inputs of selectable frequency and amplitude.
- HHC optimization panel to alter the scheduled HHC coefficients amplitude and phase a limited amount.
- Realtime and stored data acquired by the inflight data measurement system which monitors the cross channel data links and records and telemeters a predetermined complement of data.
- The program monitor and control unit (PMCU) to permit flight line interogation of the FCC for fault code readout and system diagnosis.

C. Higher Harmonic Control

In recent years requirements for reduced vibration have become stringent. Thus, it is mandatory to develop and demonstrate weight-effective, airframe vibration control. For current generation helicopters the rotor speed may be varied by large percentages, e.g., 11% on S-76, to optimize aircraft characteristics such as external acoustics and performance. This may make the use of more conventional fixed-tuned vibration control devices more challenging because of weight constraints and adverse frequency response characteristics. Analytical studies, wind tunnel tests and flight tests (References 1, 2, and 3) have demonstrated higher harmonic control (HHC) to be a viable technology for vibration control. Briefly, the concept underlying HHC is that reductions in $N\Omega$ frequency airframe vibrations can be achieved by oscillating the rotor blade in pitch at $(N-1)\Omega$, $N\Omega$, $(N+1)\Omega$ frequencies in the rotating system, where N is the number of blades and Ω the rotor speed.

The present paper describes a successful full scale open loop HHC effort on the Sikorsky S-76 at forward speeds up to 150 knots, Figure 20. This is the first demonstration of HHC on a 10,000 lb. helicopter at moderately high airspeeds compared to previous full scale testing. The flight test results demonstrate that for the 10,000 lb. S-76, HHC can substantially reduce vibration without incurring severe penalties in blade loads and rotor performance. In addition, a novel way of implementing the higher harmonic control other than through the conventional swashplate is also described.

Vibration Characteristics of the S-76

The S-76 is a modern medium size helicopter used mostly in the commercial market for VIP transport and offshore oil missions. For both these missions the ride quality in the cockpit and cabin is extremely good. This four-bladed rotor system is designed to minimize the 4P (4 per rev, 19.5 Hz at 100% NR) vibration in conjunction with rotating system 3P and 5P inplane bifilar absorbers with cycloidal tuning bushings. The ride quality in the forward cockpit is further enhanced by the use of a variable tuned fixed system vibration absorber. Reference 4 discusses details of the dynamic design. The self-tuning nature of the bifilars and the nose absorber allow for rotor speed operation over a 11 percent range to optimize performance. While this system works well, it requires 2.75% of the design gross weight. The possibility of achieving lower weights with an HHC controller makes this concept of potential interest. Additionally, while the self-tuning features of the current system allow for rotor speed variations to optimize performance, a much larger range of operating speed changes can be accommodated with HHC.

Objectives of Flight Test Program

The primary objective of the flight test program was to determine the extent of HHC open loop vibration reduction attainable in the S-76. This included simultaneous vibration reduction at several locations in the aircraft. The capability to generate vibratory blade pitch motion using the main rotor hydraulic servos, as well as the attendant change in control and rotor system loads were evaluated.

Modifications to S-76 for HHC Open Loop Flight Test

Figure 21 shows the mechanical and electrical elements of the HHC system. This figure shows the main rotor servos and the modified valves which improve the servo high frequency response. Figure 21 also shows the HHC electro-hydraulic driver actuators that were installed on the input side of the main servos. The HHC controller electronic components are shown in the top left hand side of Figure 21. Figure 22 is a schematic diagram of the modified S-76 control system. The lateral main rotor servo is not shown for clarity.

The S-76 is normally equipped with rotor head mounted 3P and 5P inplane bifilar absorbers and a nose mounted variable tuned vibration absorber. The bifilars were removed and the nose vibration absorber was turned off during the HHC flight testing. The HHC control system inputs were generated by use of the HHC control panel (Figure 21) which provides electrical signals to the HHC electro-hydraulic driver actuators.

Flight Test Data Results

Figure 23 shows the results of the HHC longitudinal cyclic mode on two vibration parameters as a function of HHC input phase angle during level flight at 80 knots. The vertical aircraft nose vibration is particularly sensitive to this HHC input and exhibits the characteristic sine wave shape that was also identified in Reference 2. This behavior may be understood by viewing the resultant vibration level as a vector sum of the baseline vibration with HHC off and the vibration induced by the HHC blade pitch oscillations. The lateral pilot overhead vibration, by comparison, is not as sensitive or as well behaved relative to the HHC longitudinal cyclic mode input.

Figure 24 illustrates the maximum cockpit vibration reduction attained with HHC. Note that the magnitude of HHC vibration reduction is essentially constant with airspeed. The vibration levels in the cockpit with HHC are generally less than .10 g's up to 100 knots, but then begin to increase rapidly with airspeed.

This behavior is due to an upper limit on the magnitude of HHC blade pitch that can be generated with the existing hydraulic pump capacity. There is little doubt that larger higher harmonic blade pitch angles would allow the vibration level to be reduced to less than .10 g's at higher airspeeds. Similarly, Figure 25 shows a comparison of vertical aircraft nose vibration during climb, partial power descent and turns. These data were obtained by using the optimum HHC setting determined for level flight and this setting was then held constant during the maneuver. Note that during the 45 degree and 60 degree angle of bank turns the vibration reduction due to HHC is essentially the same as that attained during level flight. It is expected that even greater vibration reductions could be achieved with larger HHC blade pitch motions.

Structural data from the HHC flight testing show that control system vibratory loads generally increase with HHC input. An example of this is the plot of pushrod vibratory load versus airspeed, which is shown in Figure 26. The HHC input for these data corresponds to the longitudinal mode input, utilized to minimize vertical aircraft nose vibration. It should be noted that although pushrod vibratory loads are increased by the use of HHC, they are still well below the endurance limit. The effect of HHC blade pitch oscillations on main rotor blade, flatwise vibratory bending moments is illustrated in Figure 27. Again, the loads generally increase due to HHC, but are not large enough to be limiting.

Figure 28 is a plot of main rotor torque versus airspeed, which represents the level flight performance of the aircraft with HHC on and off. The HHC input is the same longitudinal mode input described in the preceding paragraph. These data were obtained by maintaining the HHC setting constant in level flight. A data record was then taken with HHC off and then one with it on. A comparison of the main rotor torque reveals no significant performance change due to HHC in level flight over the speeds for which performance data were obtained.

Oscillating Jet Flap

One method for implementing higher harmonic control for helicopter rotors is to produce time-varying pitching moments using a pulsating jet flap. These pitching moments would induce blade torsional oscillations to control blade loading and therefore reduce airframe vibration. The advantages of this technique include having no moving parts (outside of the air supply to the jet), having low power requirements, and producing low inertial loads. In this concept the jet would exit the blade trailing edge along a section between 80 and 90% of the radius. Locating the jet exit on the lower (pressure) surface of the blade would

provide both the required unsteady torsional motion and a steady untwisting of the blade in forward flight. Use of a Coanda surface rather than a pure jet flap is recommended to increase the pitching moment response to a given jet momentum coefficient.

The aerodynamics of this technique have been studied experimentally using an SC1094-R8 airfoil that was modified to incorporate a Coanda jet at the trailing edge of the blade surface (Fig. 29). The jet exited from a 0.03-in.-high, 2-ft-wide slot located in the center of an 8-ft-wide S-76 blade section. Jet pressure and frequency were varied. Wind tunnel tests were conducted at Mach numbers of 0.4 and 0.7.

Unsteady surface pressures were measured using twenty-four miniature pressure transducers located along the airfoil centerline (Fig. 29). The normal force and pitching moment coefficients were determined by a Gaussian integration along the airfoil chord. The static pressure at the jet exit and the total pressure in the plenum inside the airfoil were used to determine the jet momentum coefficient. Figure 30 presents a representative time history of this coefficient.

One example of the results is shown in Figure 31. The mean (time-averaged) pressure distribution is characterized by a peak in -Cp in the jet region on the pressure surface. The pressure amplitude at the fundamental jet frequency is also highly peaked in the jet region. The phase of the pressure on each surface increases slightly with distance from the leading edge of each surface, and maintains a 180 degree phase separation between the surfaces.

Loops showing the variation of the pitching moment about the quarter chord with jet momentum coefficient are shown in Figure 32 for jet frequencies of 5 and 25 Hz. The primary difference between the two curves is the increased hysteresis at 25 Hz for low values of momentum coefficient. Figure 33 shows the variation of the amplitude of the normal force and pitching moment coefficients at M = 0.4 with jet frequency, mean angle of attack, and regulator pressure. The data appear self-consistent, and, especially at the higher pressures, to vary smoothly as a function of all three independent variables.

One of the primary results of this study is shown in Figure 34. This figure shows that the pitching moment amplitude is nearly a linear function of the jet momentum coefficient amplitude. The slope does not seem to change greatly with angle of attack or reduced frequency. The predictable and generally well behaved aerodynamic response demonstrated in this experiment indicate that it would be feasible to generate rotor control moments using the

oscillating jet flap concept. The relationship between the normal force and pitching moment and the momentum coefficient for these very low flow rates are proved to agree with predicted values thus confirming that adequate higher harmonic vibratory pitch could be provided with the predicated low power levels.

Key Design Issues Associated With Implementation of HHC at Higher Airspeeds

HHC Amplitude at Higher Airspeed

During the S-76 HHC flight test it was found, as expected, that the amplitude of the higher harmonic blade pitch was limited by the hydraulic fluid flow capacity. It is expected that higher amplitudes of the blade pitch would lead to further reductions in hub loads (main rotor shaft bending moments) and consequently further reductions in airframe vibration. Blade root pitch measurements during the flight test showed that the optimum blade pitch for best vibration reduction was primarily composed of the 3P component and that the maximum amplitude of this 3P component obtained with the present hydraulic system was approximately ±1°. Implementing HHC in aircraft in approximately the same weight class as the S-76 but at higher operating airspeeds would require HHC blade pitch amplitudes in excess of ±1°. Both analysis and a semi-empirical method based on flight test data project that ±2° of high harmonic blade pitch amplitude would be required for an S-76 operating at an airspeed of 150 knots.

Weight Considerations

The weight of the present open loop HHC system in the S-76 is 75 lbs this figure represents the mechanical and electrical components that were installed in the S-76. The basic philosophy behind the S-76 HHC flight test was to design and test a prototype system as "proof of concept" with minimum change to the aircraft. In line with this objective, additional hydraulic hardware that would have been required to obtain higher harmonic blade pitch amplitudes larger than 1° was not installed. To increase the HHC amplitude to, say, ±2° would require a longer primary servo stroke (at 4P), thus requiring larger hydraulic fluid flow rates which in turn would require installation of larger capacity pump(s), reservoir(s), and cooling system(s). It has been estimated that such an HHC system would weigh 115 lbs.

Hydraulic Power Considerations

The hydraulic power requirement would depend upon whether the HHC system was operating in the collective or the cyclic mode. In the collective mode all three main (primary) servos would operate (at 4P) with the same displacement and phase; this mode of operation consumes the maximum hydraulic power. In the longitudinal cyclic

mode, only the fore and aft primary servos would be active (at 4P), whereas in the lateral cyclic mode only the lateral servo would be active (at 4P). Thus the lateral cyclic mode requires minimum hydraulic power. However, it was observed during the flight test that this mode by itself was not as effective in suppressing airframe vibration as the other two modes. Hence, in the following estimates only the collective and longitudinal cyclic modes are considered. The hydraulic power requirement per stage (there are two stages in the S-76 hydraulic system) is given by

$$\text{Horse Power} = NP_s\ (2\pi f)\ (X_{RMS})\ (A)\ (\tfrac{1}{C_1})(\tfrac{1}{C_2})$$

where

N	=	number of servos active
P_s	=	hydraulic supply pressure, psi
f	=	frequency of operation, (4P), Hz
X_{RMS}	=	servo piston stroke, in, RMS
A	=	piston area, in^2
C_1	=	1714 (gallons per minute)(psi)/(HP)
C_2	=	3.85 (in^3/sec)/(gallons per minute)

Substituting typical values for the various parameters in the power expression gives, conservatively, the total HHC hydraulic power requirement in the collective mode to be 144 horse power and in the cyclic mode to be 40 horse power. The fuel associated with this power would, of course, add to the effective weight of an HHC system.

Seal Life

Another area of concern in implementing HHC on a production aircraft is the life of the seals in the main rotor servos operating at the high frequencies associated with HHC. Two S-76 servos were set-up for testing. The test spectrum consisted of a four segment spectrum of 40 minutes duration, with 10 minute segments. The test centers around the 4P frequency with a low frequency (0.5 Hz) signal superimposed to represent AFCS (automatic flight control system) signals. The first test was terminated after 550 hours and 50 million HHC cycles. No leakage or unusual wear could be observed. The units were disassembled and the seals in both servos were found to be in very good condition. Move extensive test would be needed to fully qualify the system. Jet flap could alleviate this concern, however, it would complicate the blade design.

Closed Loop HHC

Implementation of closed loop HHC in the S-76 has been considered and several key issues have been identified. Of these, the type of control law is perhaps the most important and will be discussed briefly. There are several types of control laws that can be used in a closed loop HHC system and these range from the real time self adaptive to the gain scheduling, e.g., Reference 5. The most recent closed loop investigation (Reference 6) demonstrates that a fixed-gain feedback control law can effectively suppress rotor hub loads. This is in contrast to other efforts (Reference 5, for example) where an adaptive controller was required for vibration suppression. The results of Reference 6 are encouraging because a fixed gain control law provides faster response due to less computations required to obtain an optimal HHC input compared to an adaptive control law. Also, Reference 6 notes that fixed gain control laws can be expected to be robust whereas adaptive controllers may be subject to instabilities.

Concluding Remarks

Open loop HHC has been successfully demonstrated at speeds up to 150 knots in a 10,000 lb aircraft. Substantial reductions in airframe vibration were attained; even higher reductions are possible by increasing the amplitude of the higher harmonic blade pitch which was limited by the current aircraft hydraulic system.

The test data show that HHC increases the pushrod loads and generally increases the blade loads. These increases, however, are not large enough to be limiting.

A novel idea of providing HHC to the blades has been explored through wind tunnel tests and proved to be conceptually feasible. The oscillating jet flap has been predicted to have low power consumption and likely reduction in weight.

References

1. Bell Helicopter Company. "An Experimental Investigation of a Second Harmonic Feathering Device on the UH-1A Helicopter". U.S. Army Transportation Research Command, Fort Eustis, Virginia, TR62-109, June 1963.

2. Wood, E.R., Powers, R.W., Cline, J.H., and Hammond, C.E. "On Developing and Flight Testing A Higher Harmonic Control System", Presented at the 39th Annual Forum of the American Helicopter Society, St. Louis, Missouri, May 1983. Also, Journal of the American Helicopter Society, January 1985, Volume 30, No. 1.

3. Walsh, D., "Flight Test of an Open Loop Higher Harmonic Control System on an S-76A Helicopter", Presented at the American Helicopter Society 42nd Annual Forum and Technology Display, Washington, D.C., June 1986.

4. Niebanck, C., and Girvan, W., "Sikorsky S-76 Analysis, Design and Development for Successful Dynamic Characteristics". Proceedings 34th Annual Forum of the American Helicopter Society, Washington, D.C., May 1978.

5. Molusis, J.A., Hammond, C.E. and Cline, J.H. "A Unified Approach to Optimal Design of Adaptive and Gain Scheduled Controllers to Achieve Minimum Helicopter Rotor Vibration". Proceedings of the 37th Annual Forum of the American Helicopter Society, New Orleans, La., May 1981; Journal of the American Helicopter Society, April 1983.

6. Shaw, J., Albion, N., Hanker, E.J., and Teal, R.S. "Higher Harmonic Control: Wind Tunnel Demonstration of Fully Effective Vibratory Hub Force Suppression". Proceedings of 41st Annual Forum of the American Helicopter Society, Fort Worth, Texas, May 1985.

ROTOR PERFORMANCE IMPROVEMENTS

ANHEDRAL TIP FLIGHT EVALUATION

In 1977-1980 Sikorsky Aircraft conducted an in-house program to design, fabricate, and evaluate the effect of a swept, tapered, full-scale, anhedral tip design on hover performance and noise of the UH-60A BLACK HAWK main rotor. This new tip was designed to be interchangeable with the standard tip cap with only minor modifications to the tip cap joint. The resulting advanced rotor system is shown in Figures 35 and 36 mounted on Sikorsky Aircraft's 10,000 hp whirlstand.

The results of whirlstand tests, which were conducted in the first quarter of 1980, were most encouraging. Not only was hover thrust for a constant rotor power input increased more than 1.8% over the operating envelope comparing the anhedral tip blade with the standard blade, but rotor noise was also reduced 2 PNdb.

The anhedral tip combines the feature of anhedral (droop) with planform taper and compound sweep. The remaining features of the production tip, namely spanwise twist and airfoil section are retained. The fundamental basis for "drooping" the blade tip is to alleviate the interference effects of the tip vortex by increasing its separation from the other blades in the rotor system. By drooping the blade tip, the tip vortex is shed lower into the rotor wake. As the tip vortex extends rearward toward the next following blade, it then passes farther below that blade. The resulting local flow distortions at the following blade are significantly reduced and rotor power and noise are beneficially affected. This tip concept is applicable to most helicopters.

In 1981 a full-scale flight test program to evaluate the prototype anhedral blade tips on a prototype YEH-60B aircraft was initiated. This program was jointly sponsored by the Applied Technology Laboratory, USARTL (AVRADCOM), the NAVAL air Systems Command, and Sikorsky Aircraft. The purpose of the program was to:

1. Define the structural environment of the modified tip and blade to augment future design efforts.

2. Substantiate free hover and vertical climb performance characteristics of anhedral tips, compared to the standard production configuration.

3. Evaluate effects of anhedral tips on level flight performance and power required.

4. Assess data acquired in tests 1 through 3 above for potential impact of anhedral tips on aircraft handling qualities.

5. Evaluate acoustic signature of the anhedral tips.

The results of the test confirmed the potential of the anhedral tip.

Figures 37 and 38 respectively present the rotor speed and load factor envelopes explored in the test as a function of calibrated airspeed. Vehicle gross weight was limited to one value by the program scope. As indicated, the anhedral tip main rotor flight envelope included an advancing blade Mach number of 0.919 and an advance ratio of 0.410, these were attained at 100% main rotor speed of 258 RPM. Rotor speeds from 90 to 110.7% Nr in auto-rotation and a load factor of 1.91 G's were recorded. The rotor remained stable for all flight conditions. The anhedral tip had no significant effect on the inboard portion of the main rotor blade, control loads, or cockpit vibration. However, the anhedral tip increased the blade flatwise stress in the area of the tip cap attachment. This was corrected by adding 5 simple stiffening clips to the affected area, which increased the strength of the tip rib and for the same loads reduced the stresses.

The hover and vertical climb data were analyzed as a function of the aircraft heading with respect to the residual winds (always less than 4 knots). This approach acknowledges wind influence on main rotor-tail rotor interference and is effective in reducing attendant data scatter. Figures 39 and 40 respectively indicate the benefits of the anhedral tip geometry observed in both flight regimes. For hover the average increase in lift capability was 2% gross weight based on main rotor power and 2.4% based on total power. Likewise the vertical climb data indicated power reductions of 2% and 1.6% at vertical climb rates of 500 FPM and 1000 FPM respectively.

Level flight results of the anhedral and standard tip performance tests are shown in Figure 41. Figure 41 presents nondimensional speed/power data and includes curve fits of the form $f(x) = Ao+A1/X+A2x^2xA3X^3$ for both the anhedral and standard tip configurations. Data are corrected to standard sea level conditions and tests for both configurations were conducted at the same referred gross weight and rotor speed. The maximum speed difference is on the order of 1 knot at constant power in the cruise speed range. A statistical T-test of the data with a confidence level of 90% shows no significant difference.

Although specific handling quality flights were not addressed in the test program, data obtained during structural and performance flying was examined for handling qualities implications. This review showed no significant impact of the anhedral configuration. Some small differences were, however, noted. Since these could become more pronounced at higher loadings, a more rigorous appraisal was recommended as a follow-on test.

As previously mentioned, one objective of the flight evaluation was acquisition of forward flight acoustic data that would compliment the hover data previously acquired on the Sikorsky whirl tower. That data showed a 2dB noise reduction in hover. The forward flight acoustic data were acquired using the microphone array and instrumentation located at the Development Flight Center's Acoustic Range in West Palm Beach, Florida. Data were acquired using microphones at 1.2 meters and 0.020 meter above ground level. Level flight passes over the acoustic range at reciprocal headings were conducted at 80, 120, and 140 KIAS.

The acoustic test data, reduced into one-third octave bands in intervals of 0.5 second and PNLTM (Perceived Noise Level Tone Maximum) and EPNL (Effective Perceived Noise Level) values, show no differences between the two sets of data at the tested flight speeds.

When measured in terms of gain in mission capability, the effect of anhedral tips on the performance of the UH-60A and its derivatives is quite dramatic. This is even more impressive when one considers that the gains are achievable through changes only in the tip cap. For the UH-60A primary mission, the takeoff ceiling can be increased by over 500 feet, or the vertical climb rate can be increased by 230 fpm, or the takeoff gross weight (i.e., useful load) can be increased by 2% (320 pounds). Also, at fixed conditions the reduced main rotor power can be used to offset power consumed by other systems such as hover infrared suppressor or an air conditioning system. The useful load increase can be used to carry added mission equipment, more payload, or additional fuel, the latter increasing mission time from 2.30 to 2.56 hours, an additional 16 minutes or 11%.

The mission and performance increment trends noted above also apply to SH-60B and to other H-60 helicopter derivatives. In addition, the SH-60B is required to perform payload deployment or sonar dipping missions where takeoff gross weight is restricted due to a midpoint hover requirement. Application of the anhedral tip for these missions is even more beneficial; payload is increased by up to 420 lb.

3RD GENERATION ROTOR AIRFOIL DEVELOPMENT AT SIKORSKY AIRCRAFT

Rotor Tip Airfoils

Five full scale rotorcraft airfoils (Figure 42) were tested in March and April 1982 in the NASA Ames Eleven-Foot Transonic Wind Tunnel for full scale Reynolds numbers at Mach numbers from 0.3 to 1.07. The models, which spanned the tunnel from floor to ceiling, included two modern baseline airfoils, the SC1095 and SC1094 R8, which have been previously tested in other facilities. Three advanced transonic airfoils, designated the SSC-A09, SSC-A07, and SSC-B08, were tested to confirm predicted performance and provide confirmation of advanced airfoil design methods.

The maximum lift coefficients at a Mach number of 0.3 for the SC1095 and SC1094 R8 were 1.37 and 1.72, respectively. The transonic airfoils had maximum lift coefficients of 1.40, 1.22, and 1.15 for the SSC-A09, -B08 and -A07, respectively. Drag divergence Mach numbers at zero lift for these airfoils were .808, .780, .833, .848 and .860. Prior to stall and drag divergence the pitching moments were generally between 0.010 and -0.015.

The airfoil analysis codes agreed well with this data, with the Grumman GRUMFOIL code giving the best overall performance correlation. The NYU Transonic Airfoil code predicted airfoil pressures and drag divergence well, but errs in the calculation of pitching moment. The Texas A&M TRANDES/TRANSEP codes show good correlation over the full range of test conditions. The AMI CLMAX code predicts the relative maximum lift coefficient of the thicker airfoils well, but fails to predict the maximum lift coefficient of the SSC-A07. The maximum lift coefficients measured in the test exceed the CLMAX code prediction and available test data from the United Technologies tunnel by about 10%.

The SSC-A09 airfoil exceeded the SC1095 airfoil maximum lift coefficient by 2% and each transonic airfoil tested showed "gentler" stall characteristics. Low lift, low Mach number drag levels ranged from .0067 to .0088. The transonic airfoils had lower drag levels than the baseline airfoils.

The transonic airfoils produced significant performance improvements at higher Mach numbers. The maximum lift of the SSC-A09 exceeded that of the other airfoils tested at Mach numbers between 0.50 and 0.74. Above a Mach number of 0.74 the SSC-A07 had superior maximum lift capability (see Figure 43). Figure 44 shows the zero lift drag for the tested airfoils. The type of leading edge camber used for the SC1094 R8 results in an early drag rise

and a drag divergence Mach number that is significantly lower than the other airfoils. The transonic airfoils maintain low drag characteristics to Mach numbers above 0.833. The drag divergence Mach number occurs at lower drag levels for the improved airfoils, providing more drag reduction than indicated by changes in drag divergence Mach number. The lift-drag ratios for the airfoils designed using modern design methods are superior to earlier rotorcraft airfoils. The airfoils in the SSC-AXX family have better maximum L/D values than the other tested airfoils (Figure 45).

High-Lift Airfoils

Several third generation high lift airfoils for rotary wing applications have been designed at Sikorsky Aircraft and Experimentally verified in the Ohio State University 6 x 22 inch transonic test facility (OSU).

The design of these airfoils was spurred when a recent investigation into possible improvements for a high speed rotor revealed potential benefits of redesigning the existing mid span airfoil, the SC1094 R8. A significant grain in rotor lift to drag ratio could be realized if the SC1094 R8 drag divergence characteristics were improved: specifically a reduction in drag creep typical of this airfoil plus an increase in the zero lift drag divergence Mach number. An examination of the SC1094 R8 for this new rotor revealed the present maximum lift coefficient for all operating Mach numbers to be adequate, but any significant reduction in its value could compromise the rotor's performance. The present third generation rotor tip airfoil, the SSCA09, has the superior drag divergence characteristics necessary, but its maximum lift levels are inadequate for the mid span region of the rotor. For these reasons an effort was initiated to design a new (third generation) mid span airfoil with maximum lift levels comparable to the SC1094 R8 values and drag characteristics approaching those of the SSCA09. Special attention was given to reducing the SC1094 R8 drag creep.

The design effort was conventional in approach in that modifications to existing airfoil designs were made and performance predicted by numerical methods, specifically GRUMFOIL for drag divergence estimates and EPPLER for maximum lift estimates.

Two ten percent thick airfoils, the SC2110 and SC2210, are the end result of the design study and were selected for testing at OSU over Mach number and angle of attack ranges capable of providing maximum lift coefficient and zero lift drag divergence values.

Figure 46 presents lift and drag experimental results for the baseline and two new designs. These results indicate that the two new airfoils maximum lift level is higher than that of the baseline airfoil for the critical Mach number of 0.4, one of the primary design goals. This is also the case for all Mach numbers greater than 0.4, however the SC1094 R8 retains its lead in maximum C_L at 0.3 Mach number. Although absolute values of maximum lift are underpredicted by EPPLER, the relative performance of the three airfoils compares well with the numerical predictions. The improvements in zero lift drag for the two new airfoils predicted by GRUMFOIL are verified by the experimental results. Large improvements in drag characteristics are obtained for both the new airfoils with drag creep reduction showing the most significant gain. Once again, absolute values of predicted drag differ from the experimental results while relative changes between airfoils are adequately predicted.

Examination of the experimental results reveals the SC2110 to be the better performer of the two new designs and is the airfoil of choice for future Sikorsky rotor applications.

Figure 47 illustrates the performance improvements obtained by the third generation airfoils. This plots maximum lift coefficient for the critical Mach number of 0.4 against zero lift drag divergence Mach number for second and third generation root and tip airfoils, plus several competitors' airfoils. The performance gains made since the first generation rotary wing airfoil, the NACA 0012, are significant and the third generation of Sikorsky airfoils has pushed the attainable rotor operating envelope to levels comparable with other present state-of-the-art airfoils. It must be noted that Figure 47 contains data obtained in facilities other than the OSU facility and are shown as flagged symbols. For this reason Figure 47 is used only as means of illustrating the performance gains produced by the design effort.

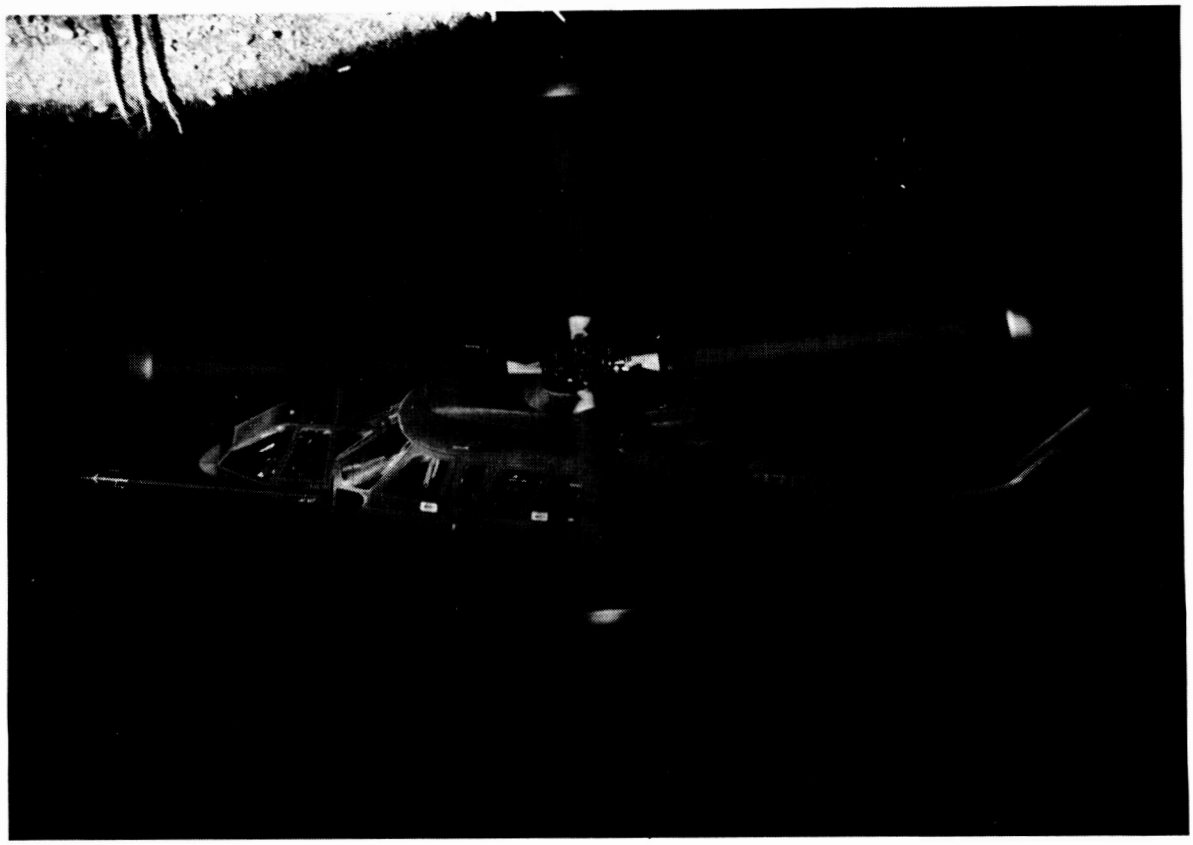

Figure 1. SHADOW Aircraft

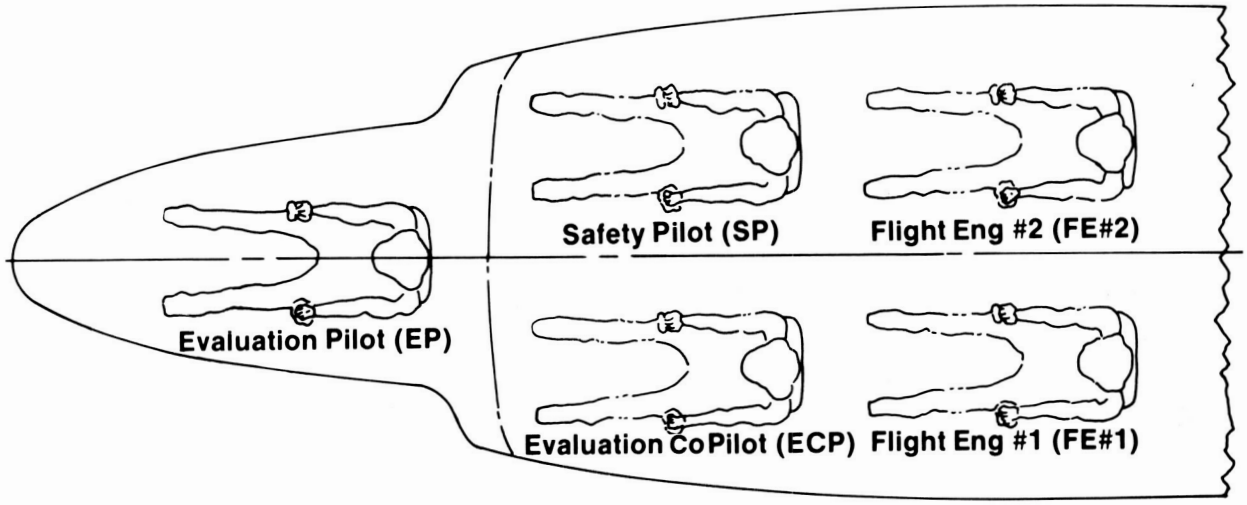

Figure 2. Crew Layout

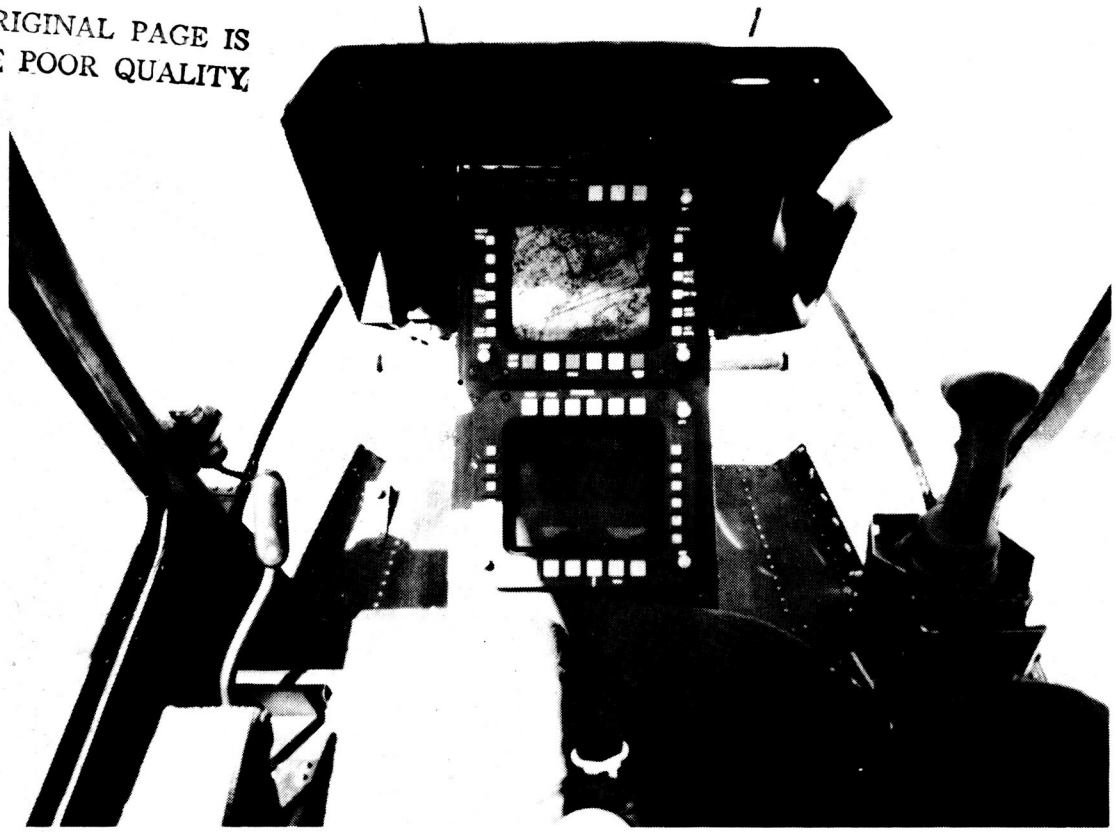

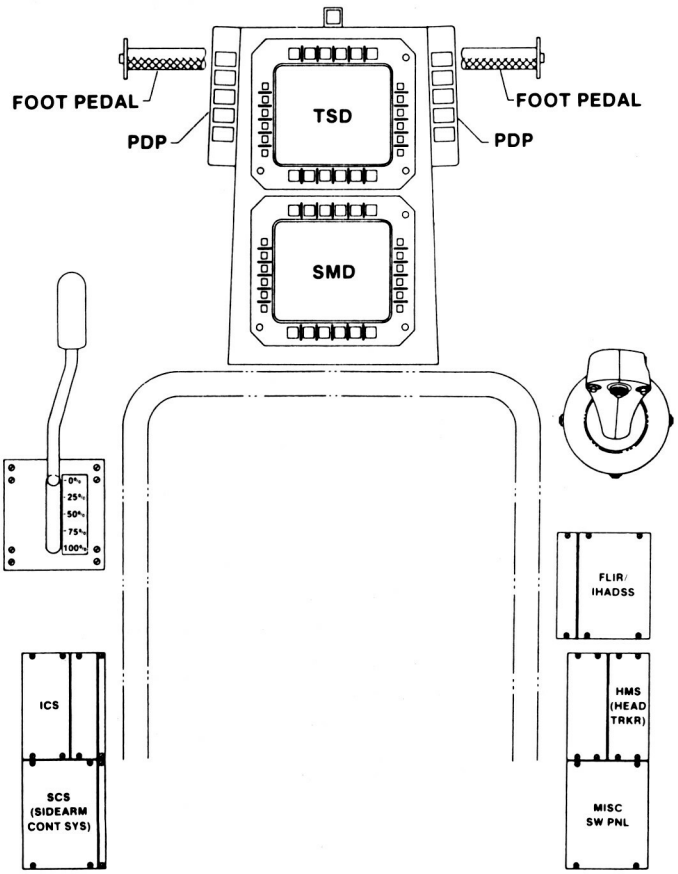

Figure 3. SHADOW Evaluation Pilot Cockpit Layout

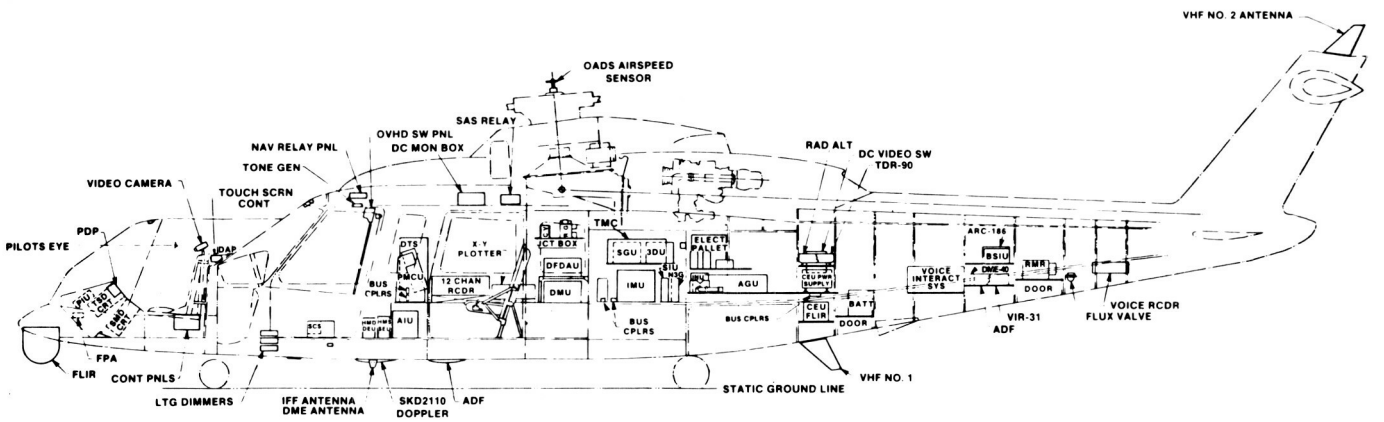

Figure 4. Avionic Layout

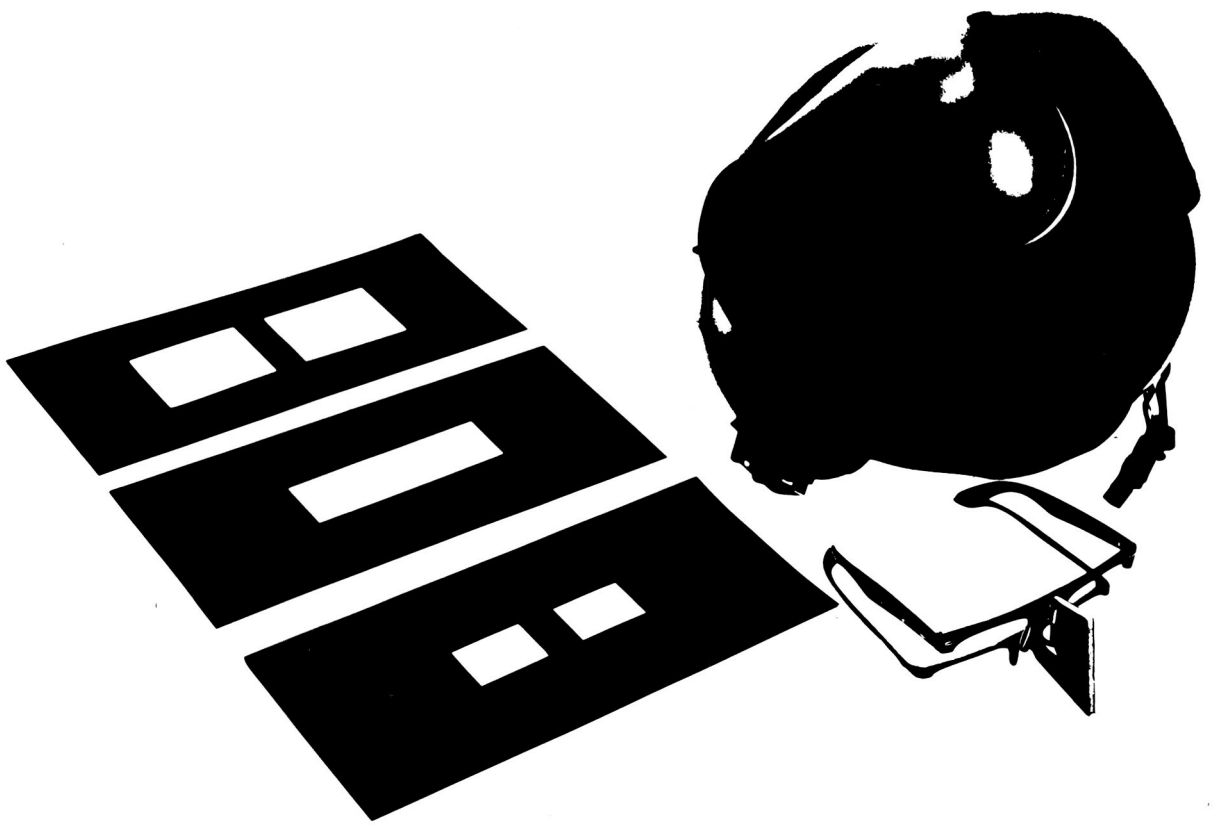

Figure 5. Photo of Three Masks, Septum and Layout

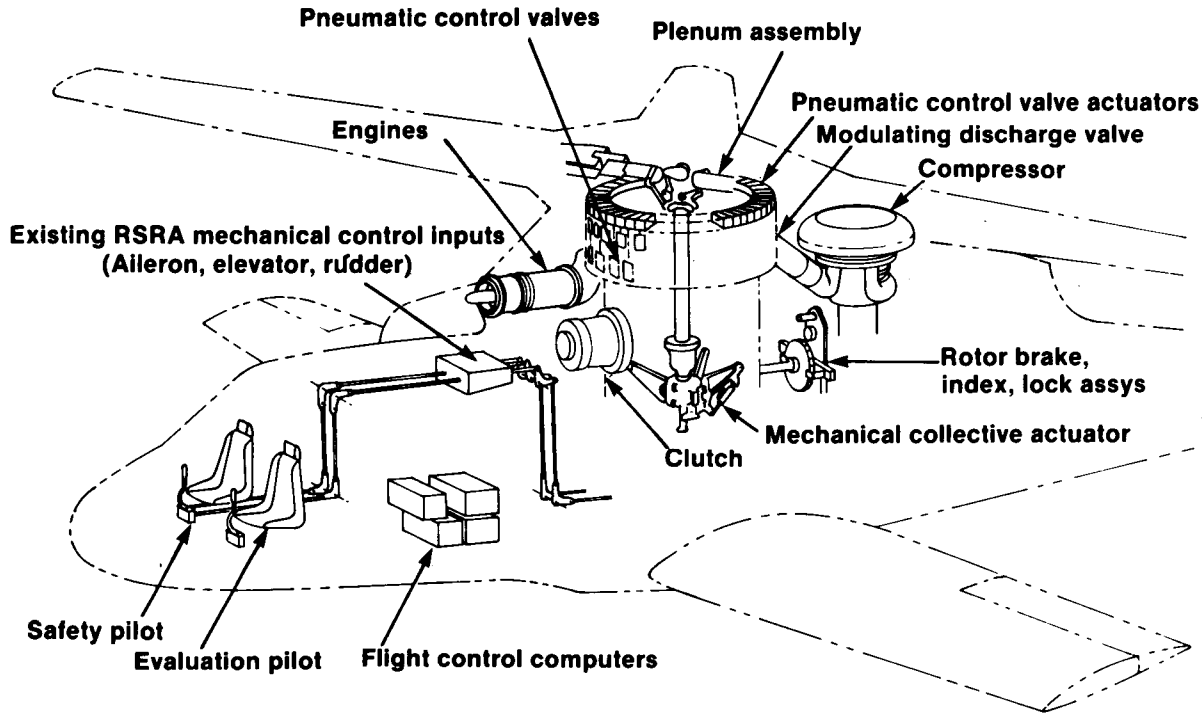

Figure 6. RSRA/X-WIng Vehicle Management System Installation

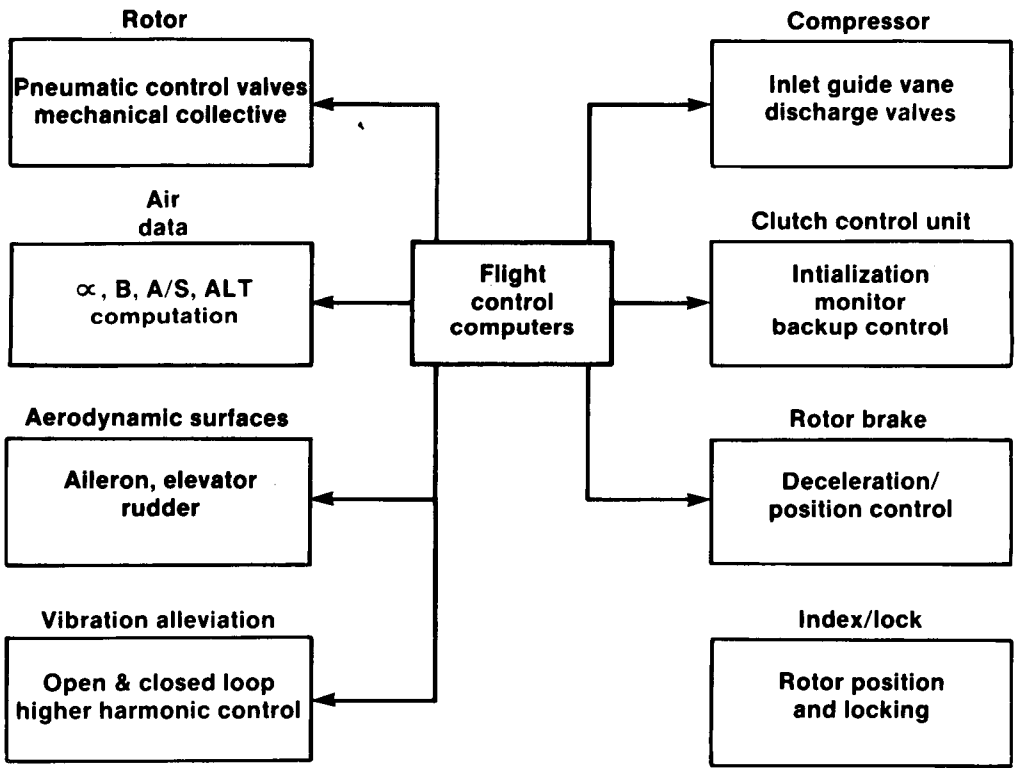

Figure 7. Vehicle Management System Functions

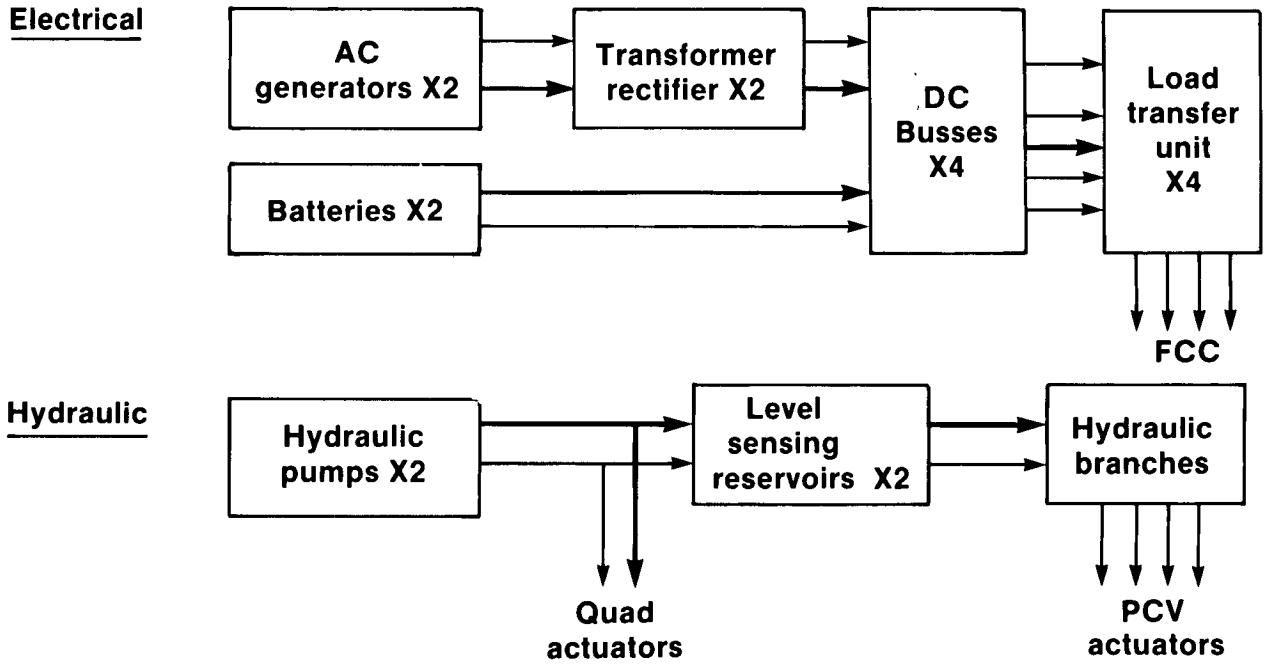

Figure 8. Power Redundancy

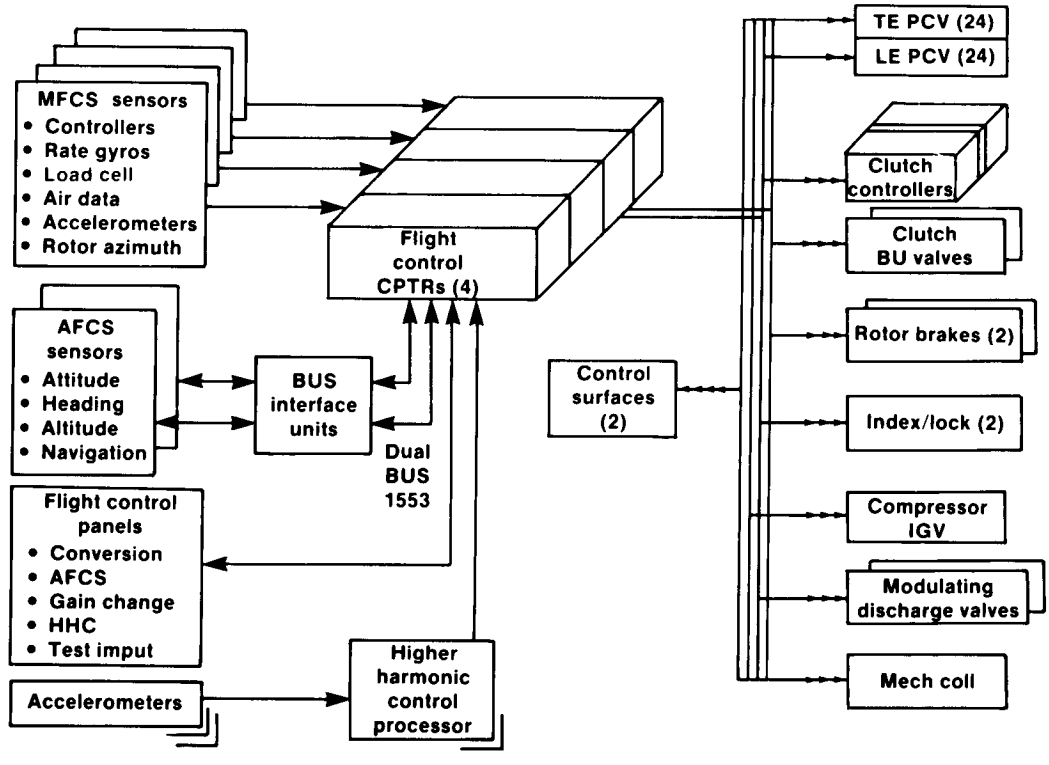

Figure 9. System Architecture

	MFCS	Direct link	Plenum dump	BUCS	Blade jettison
Full-up control laws • RW SAS • HMF	X		X		
Full redundancy	X	X	X	X	
HHC	X	X			
CCR "Blowing"	X	X			
Mechanical collective	X	X	X	X	
RSRA fixed wing controls	X	X	X	X	X

Figure 10. Control System Features Several Backup Modes

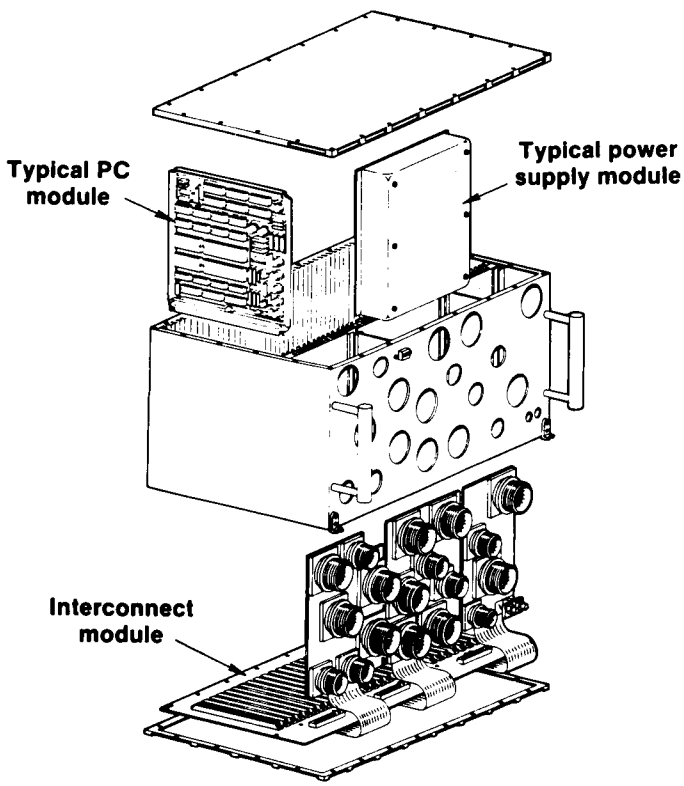

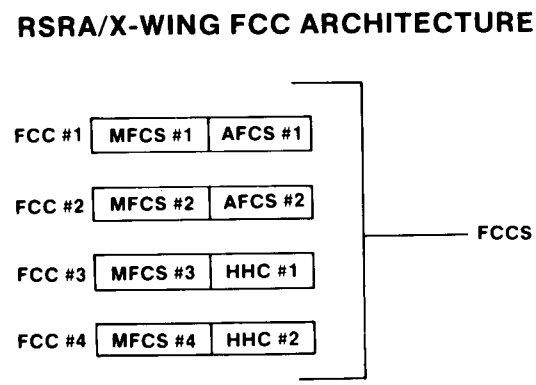

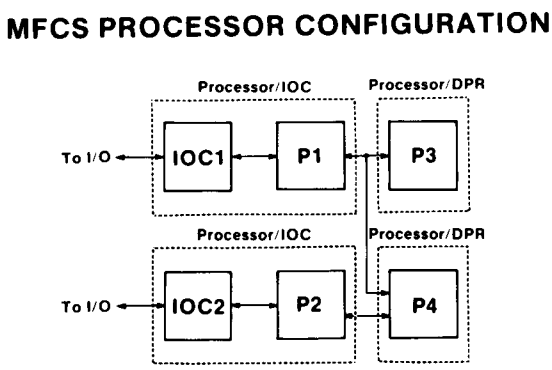

Figure 11. X-Wing FCC

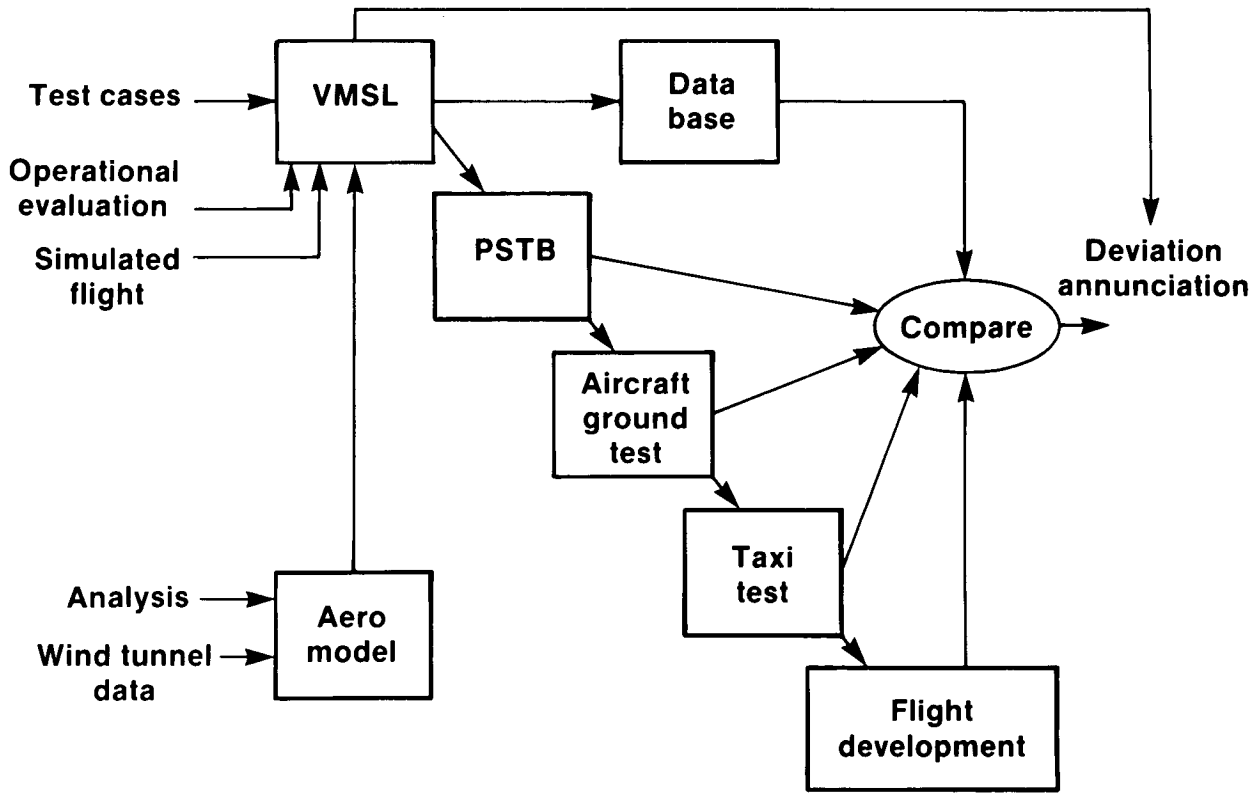

Figure 12. FCS Validation

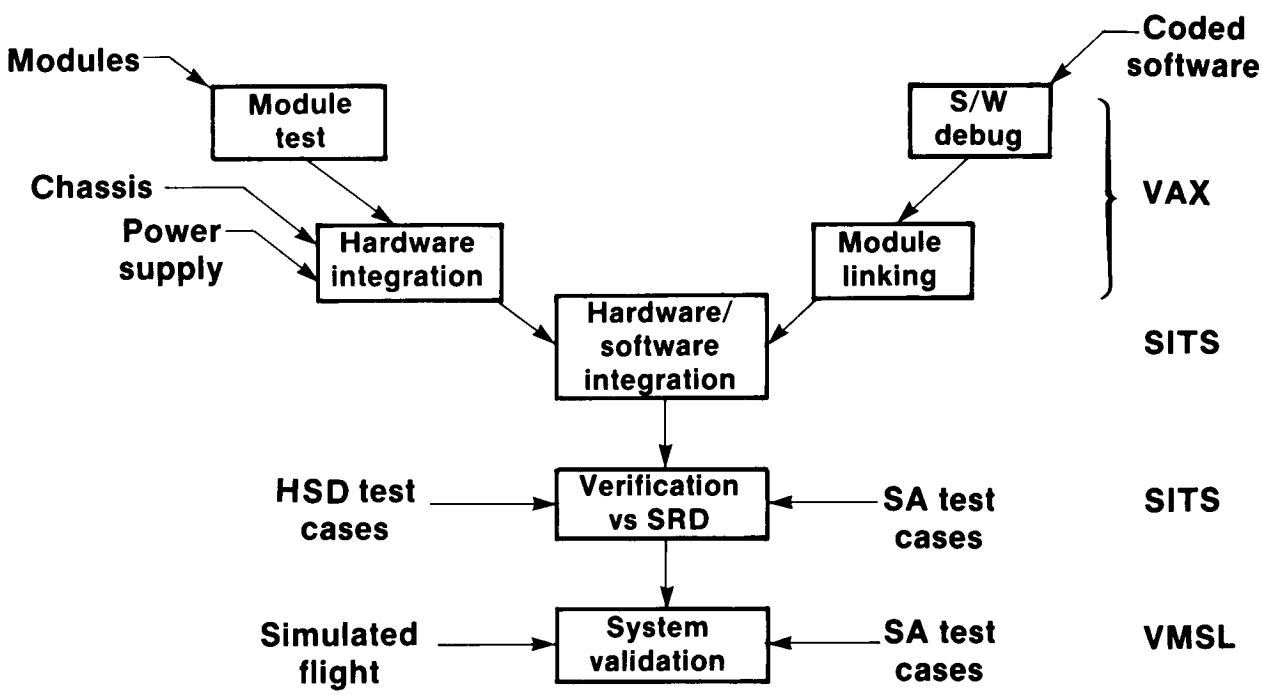

Figure 13. Flight Control System Development and Verification

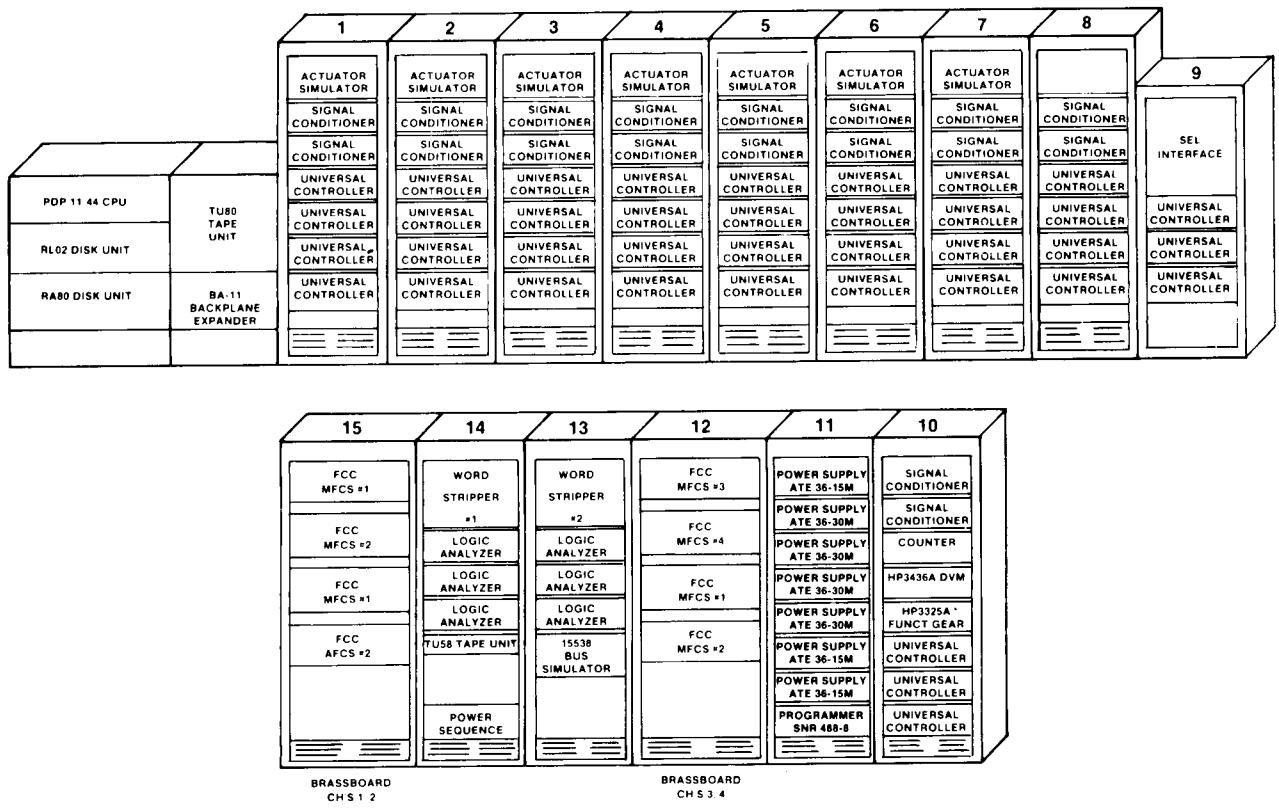

Figure 14. RSRA/X-Wing Systems Integration and Test Stand

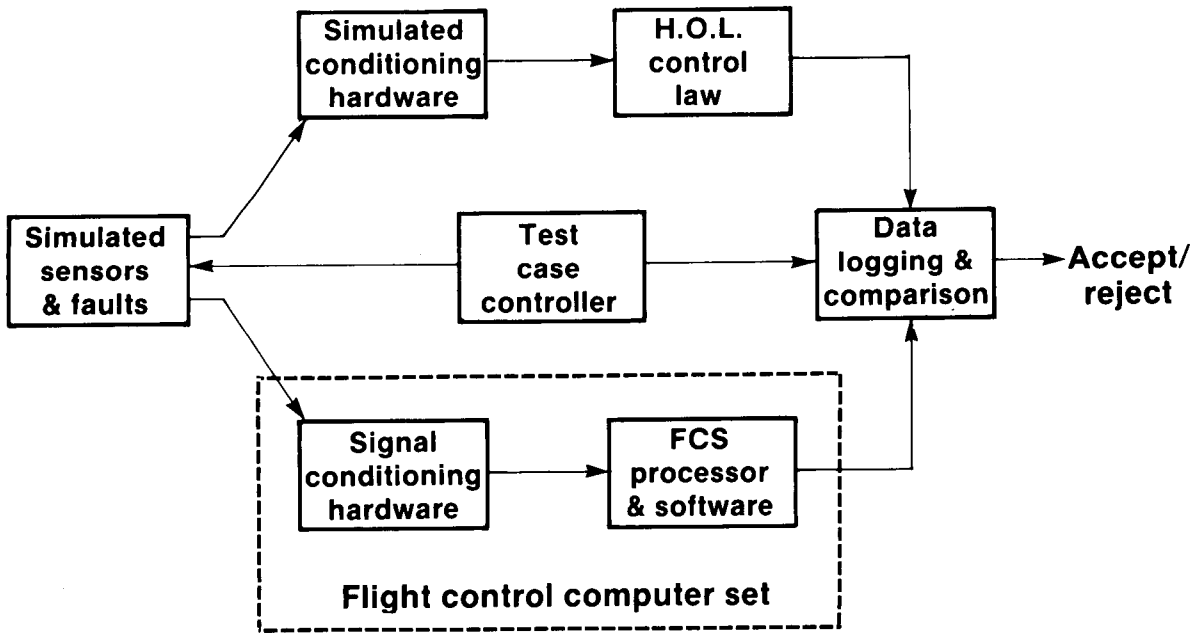

Figure 15. Automated Software Verification

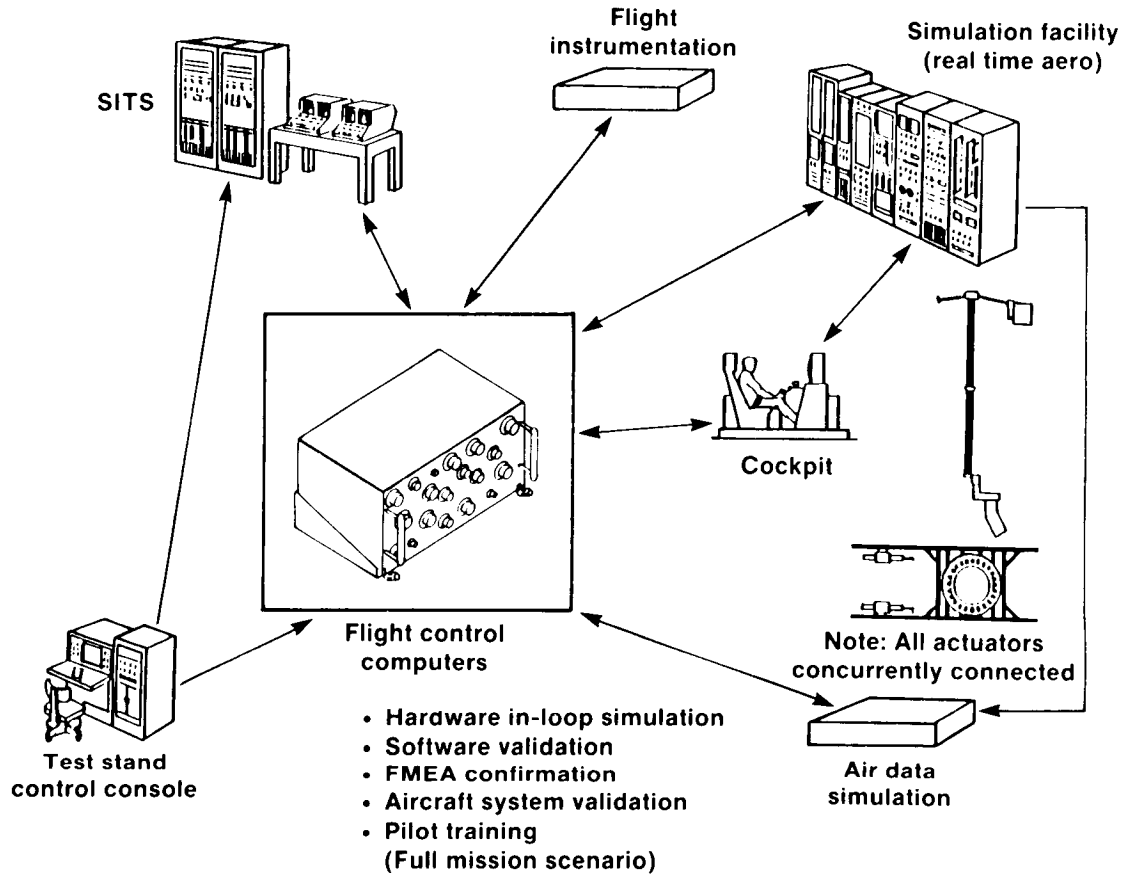

Figure 16. Vehicle Management System Lab

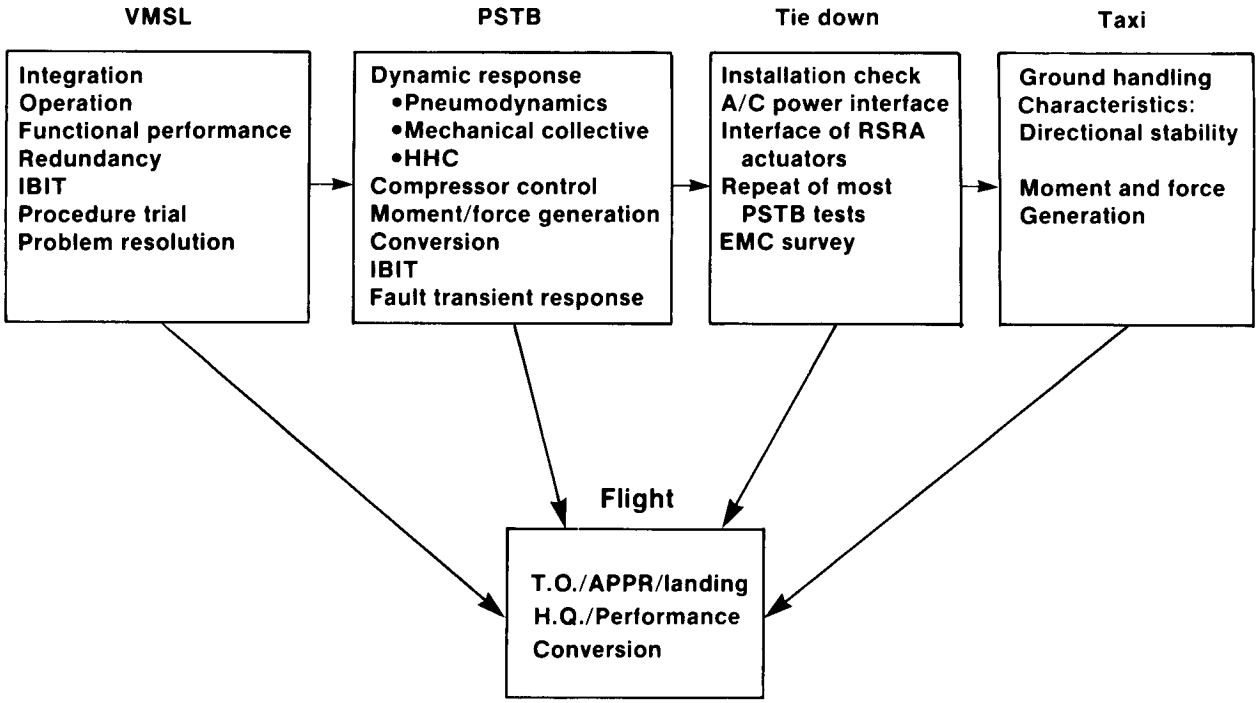

Figure 17. Validation Elements

	Rotor off	No blowing stopped	Blowing stopped	Rotary mode	Conversion
		*			
Direct Link	No FCC	No FCC	✓	✓	✓
Unified Control Laws				✓	✓
BUCS			✓	✓	✓
HHC				✓	✓
AFCS			Partial	✓	✓

* Blade feathering locked in place

Figure 18. RSRA/X-Wing Code Usage During Flight

- Reprogrammable memory
- Alternate gains
- Test input panel
- HHC optimization panel
- Realtime and stored data acquisition
- PMCU

Figure 19. System Flight Development Features

Figure 20. The Sikorsky S-76 in Flight

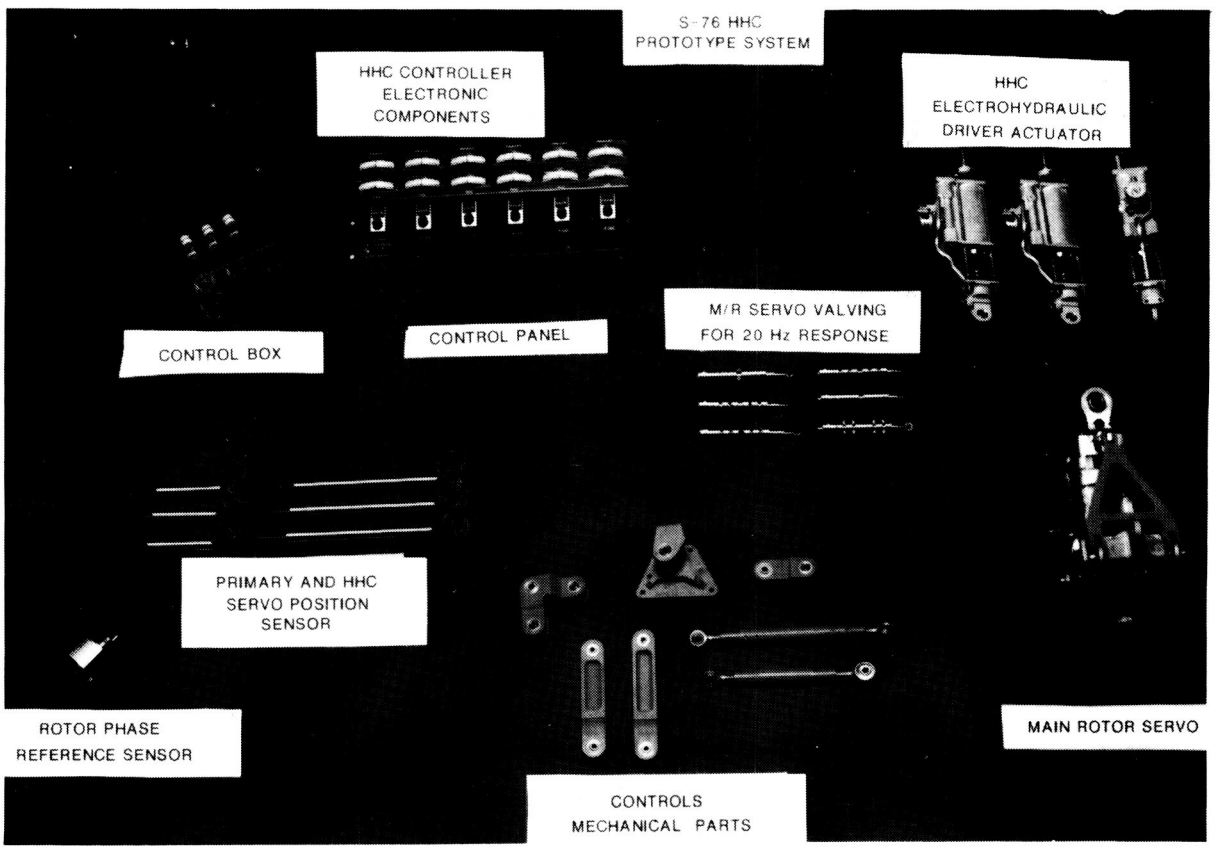

Figure 21. Mechanical and Electrical Elements of the HCC System

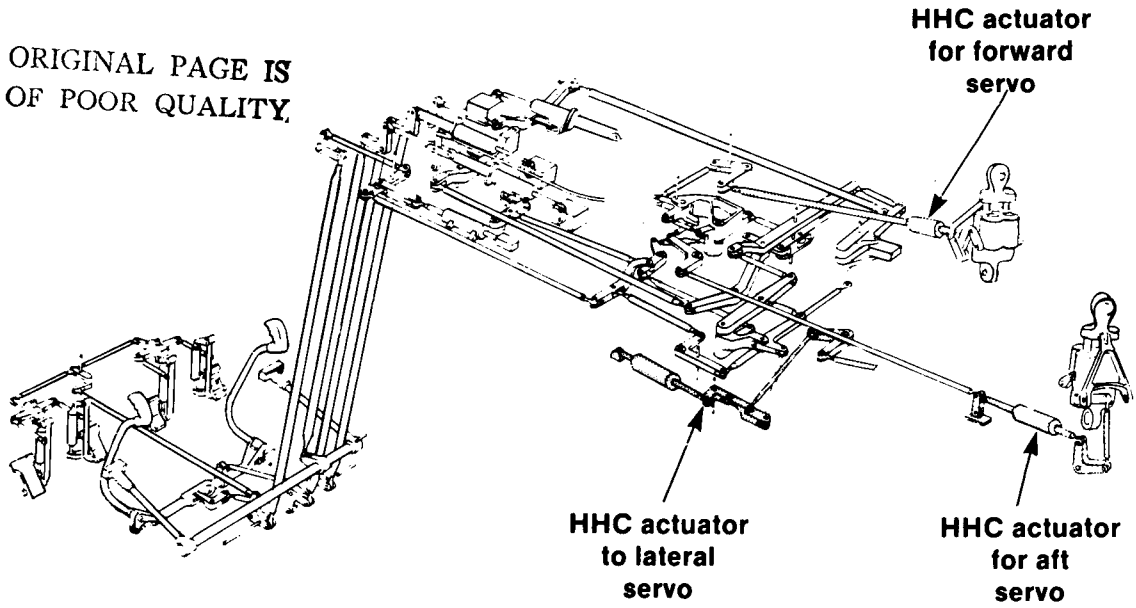

Figure 22. Schematic of HHC Modifications to the S-76 Control System

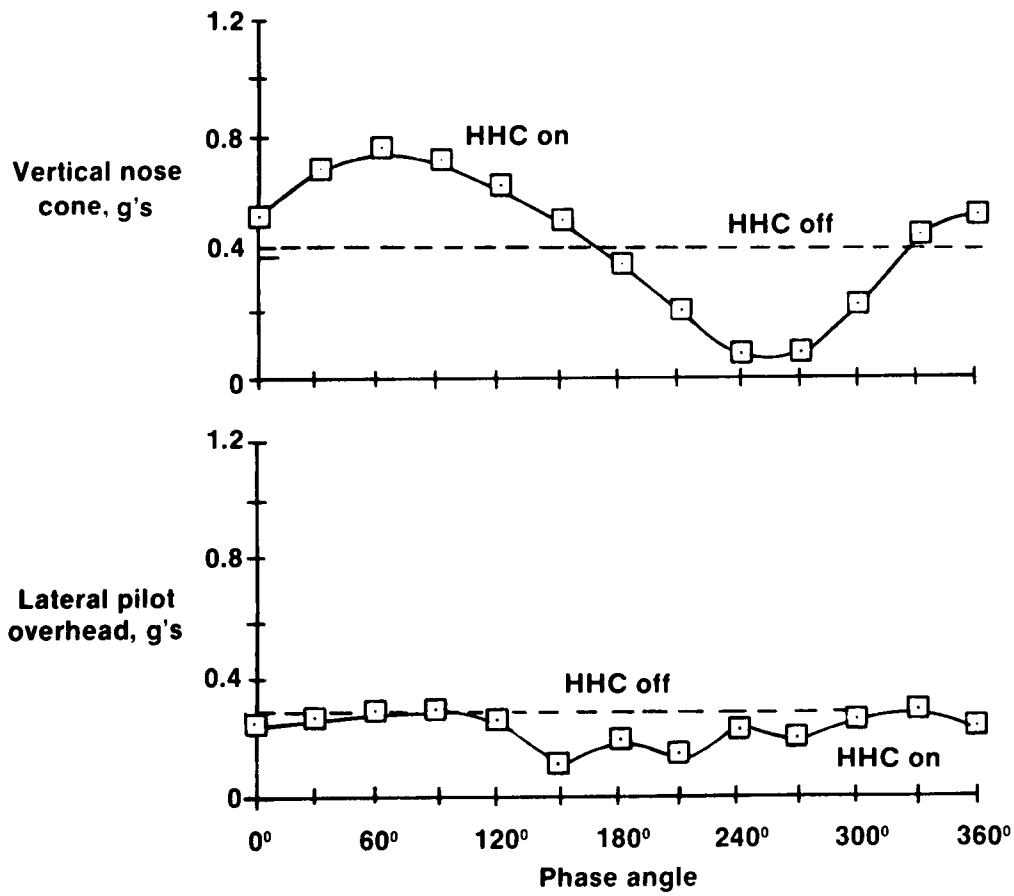

Figure 23. Effect of HHC Longitudinal Cyclic Mode on Cockpit Vibration, Level Flight, 80 Knots, 100% NR

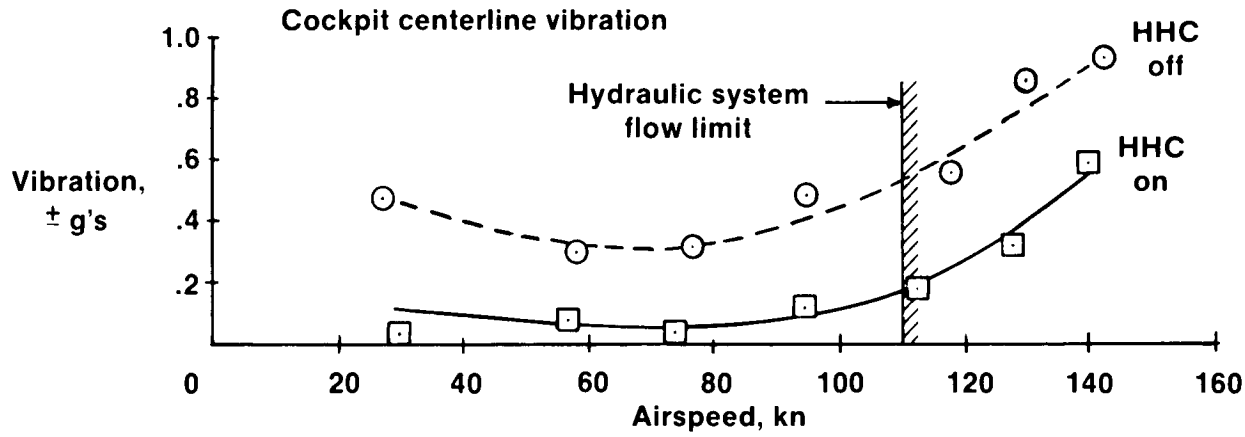

Figure 24. Reduction in Cockpit Centerline Vertical Vibration, 100% NR

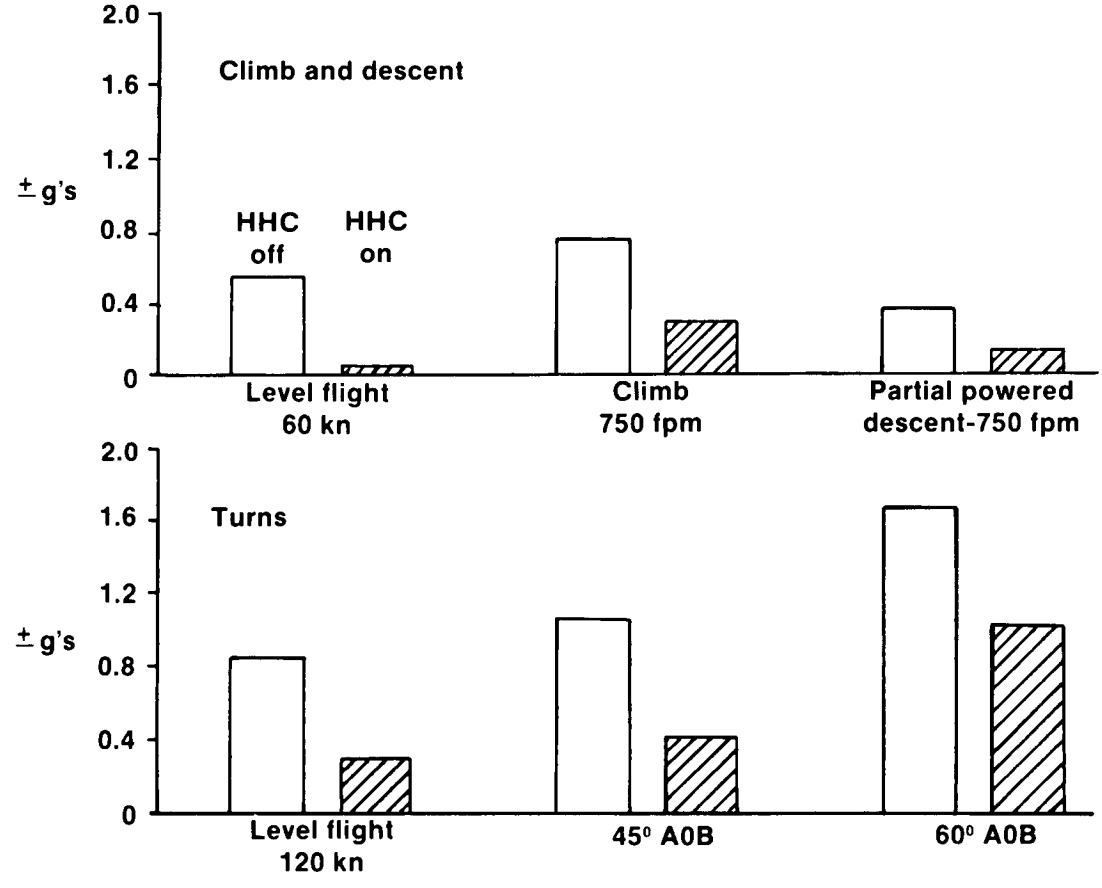

Figure 25. Reduction in Nose Vertical Vibration During Maneuvers

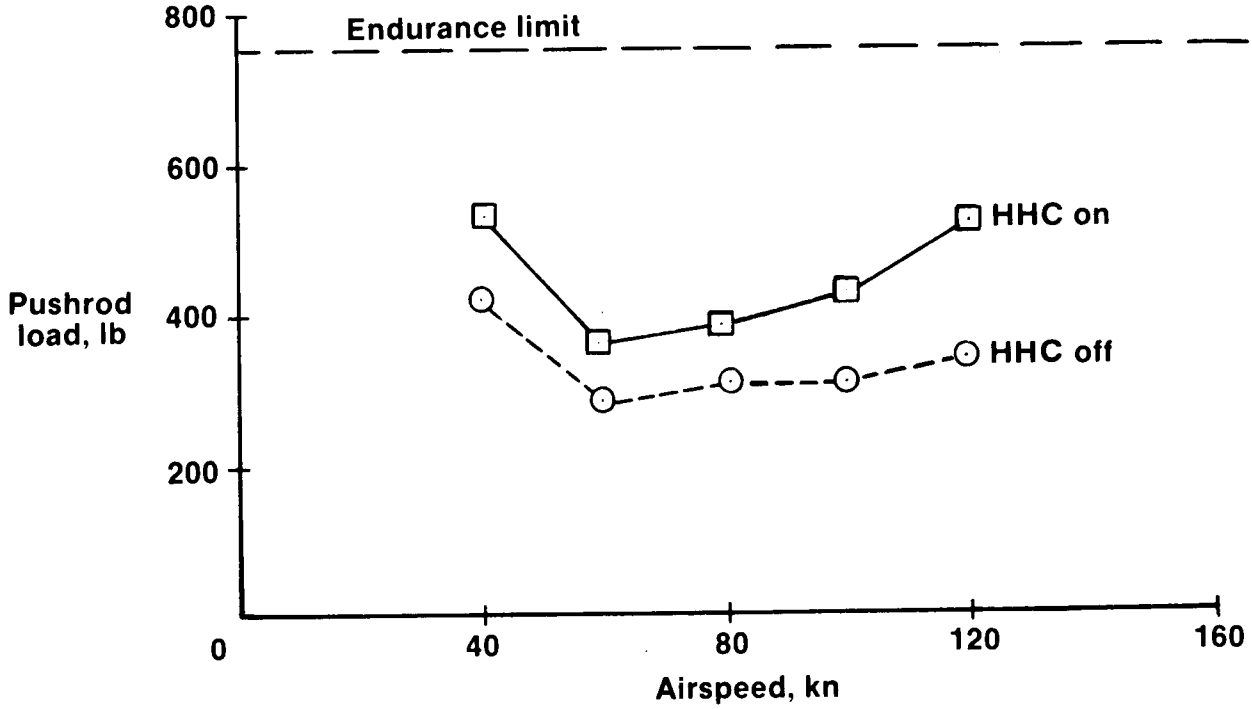

Figure 26. Effect of HHC Longitudinal Mode Input on Pushrod Vibratory Load

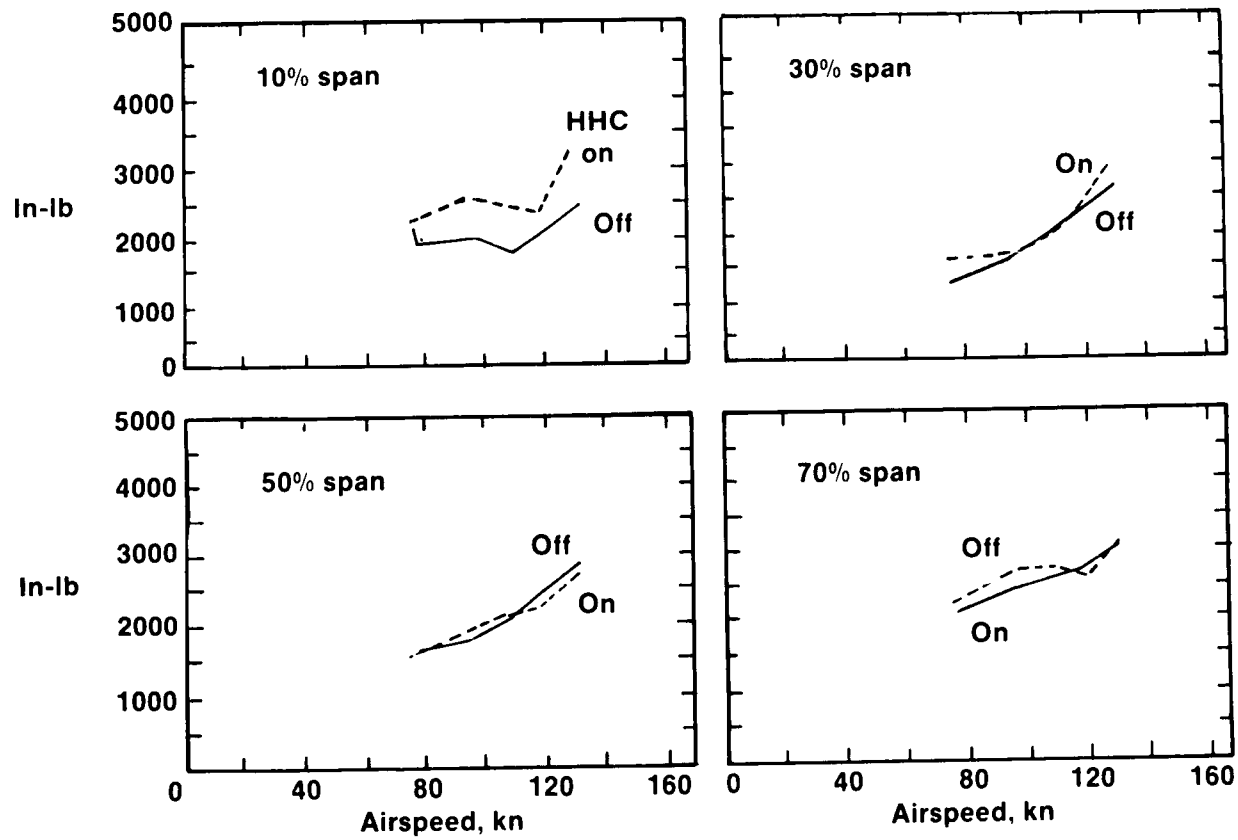

Figure 27. Effect of HHC on Blade Flatwise Vibrator Bending Moment

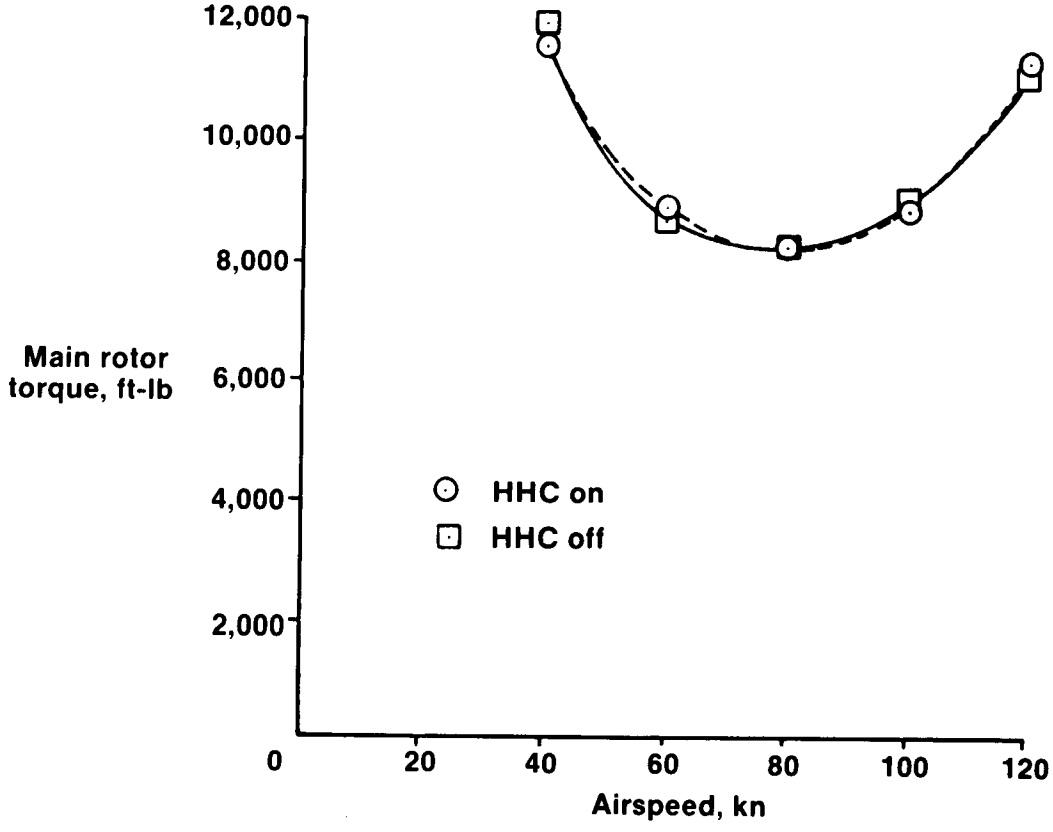

Figure 28. Level Flight Performance, Effect of HHC Longitudinal Mode, 107% NR

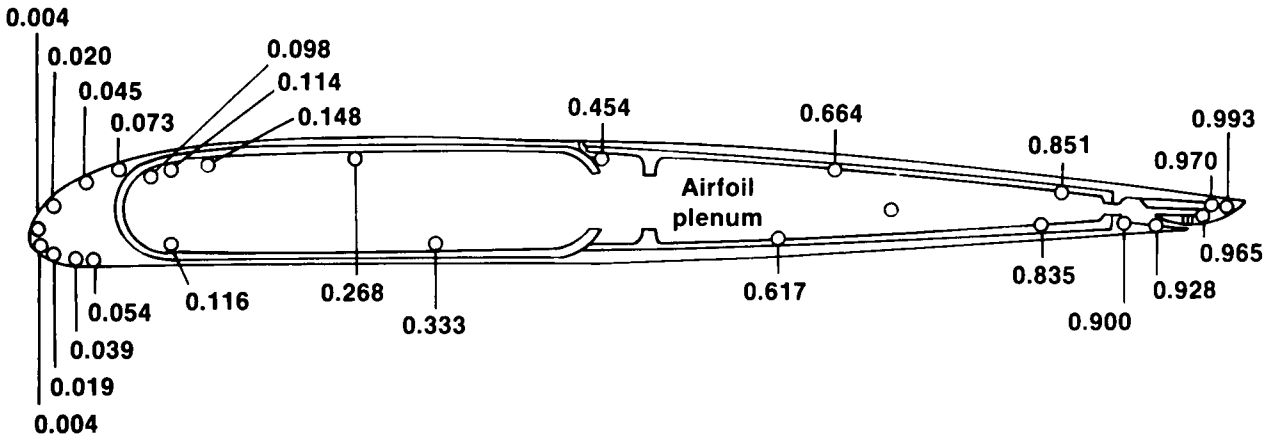

Figure 29. Airfoil Section and Transducer Locations

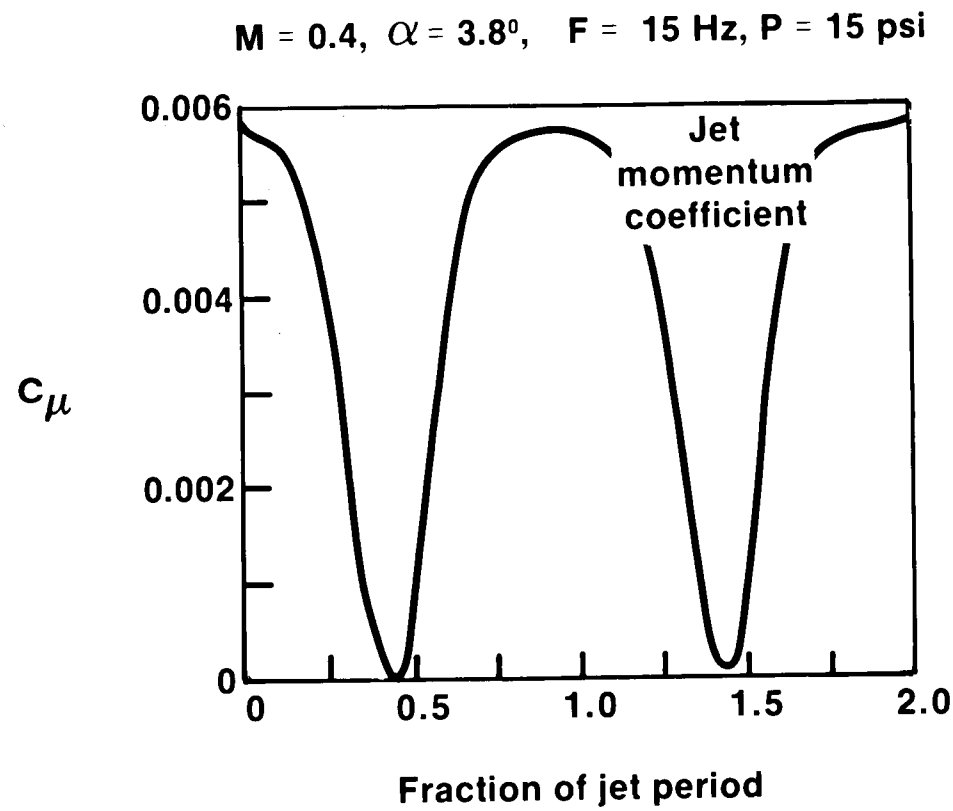

Figure 30. Time Histories for Jet

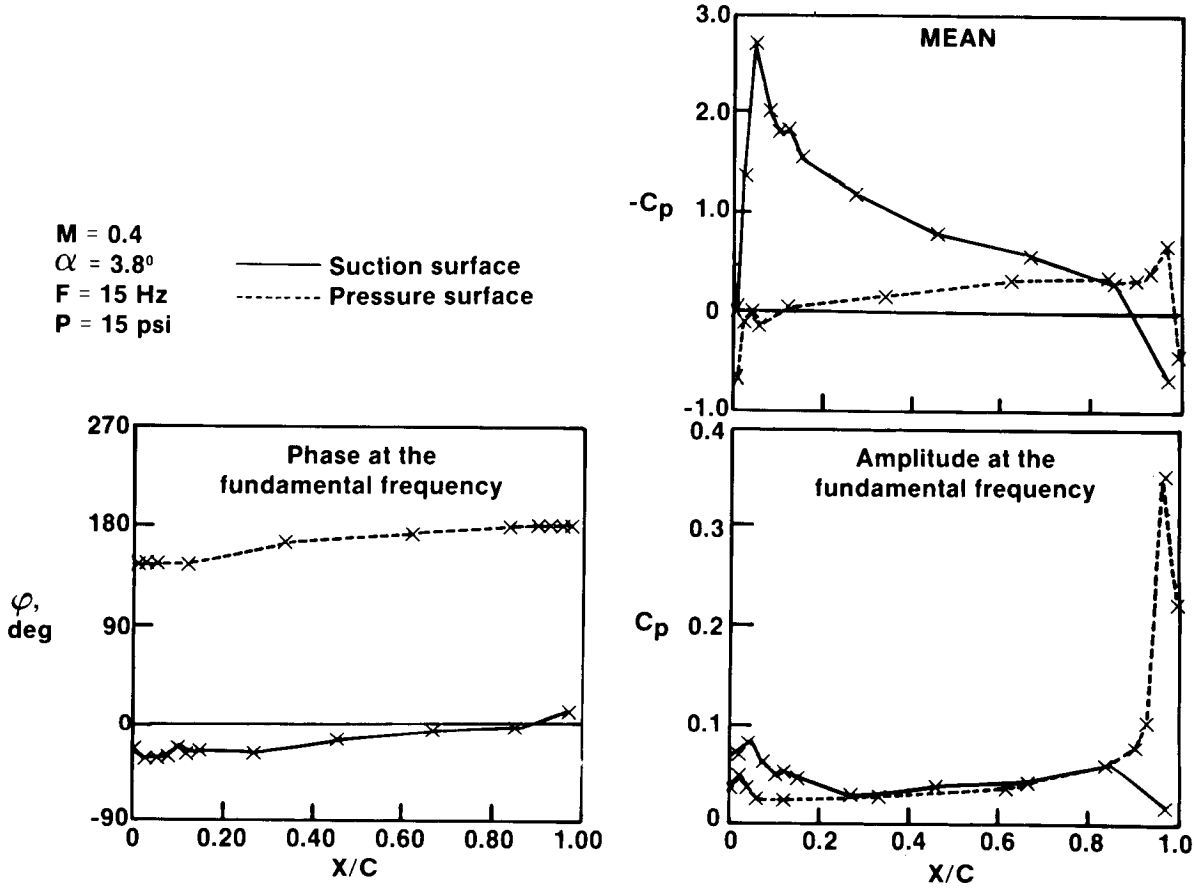

Figure 31. Surface Pressure Distributions

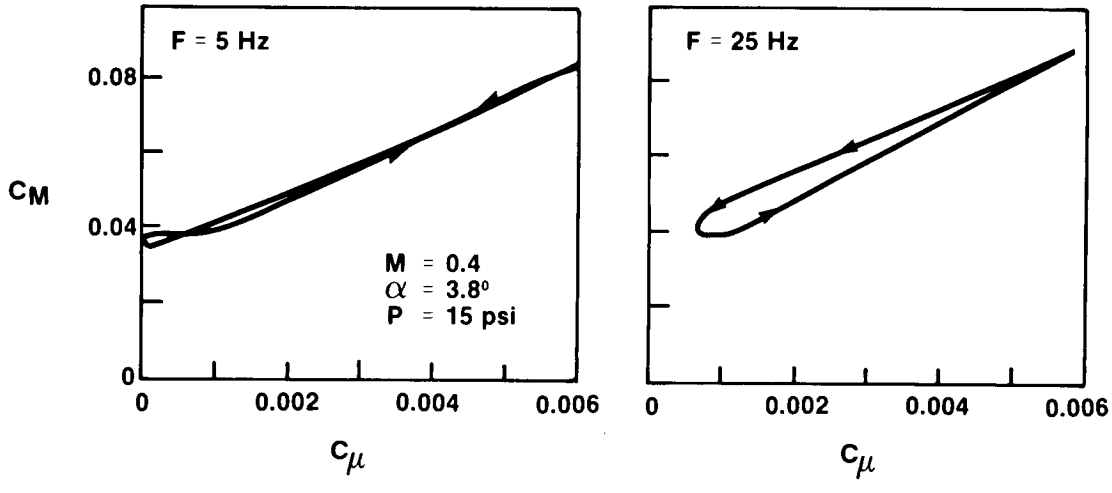

Figure 32. Loops of C_M vs. C_u

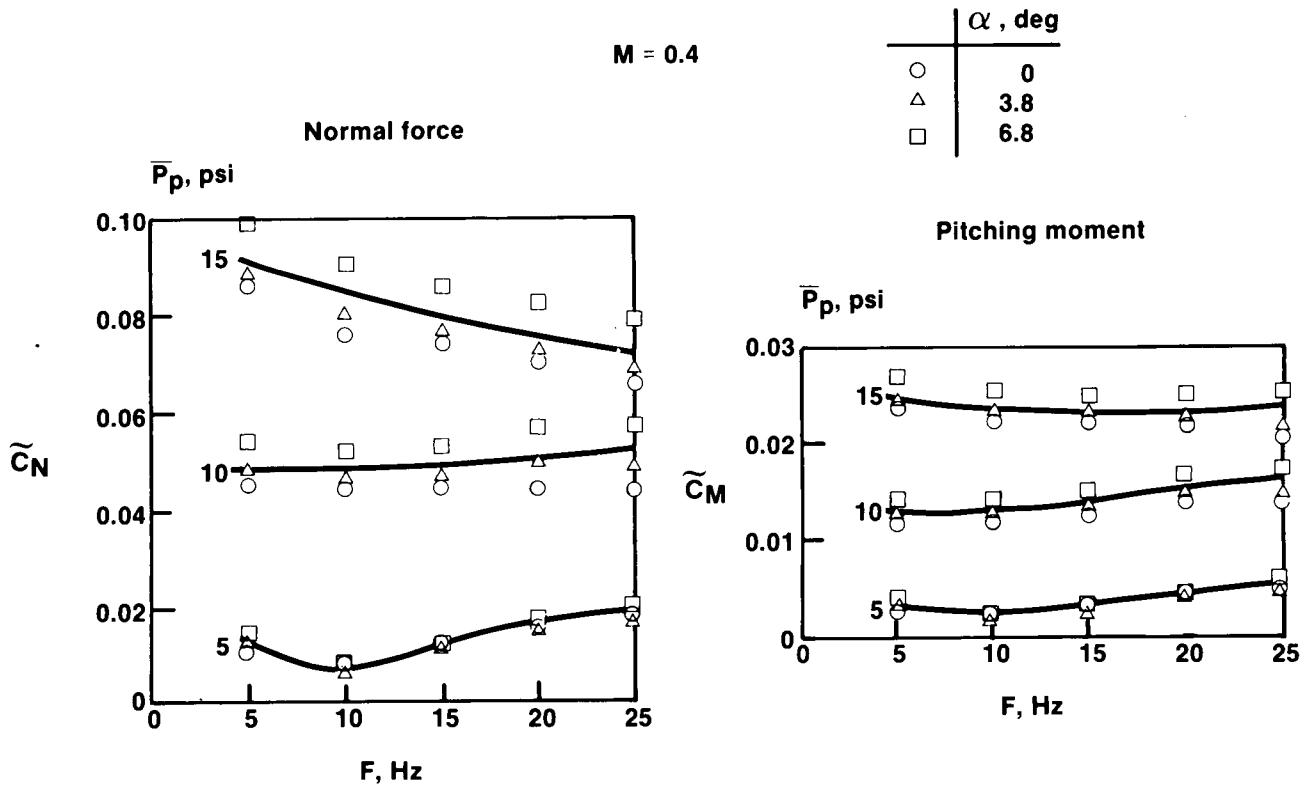

Figure 33. Fundamental Amplitudes vs. Frequency

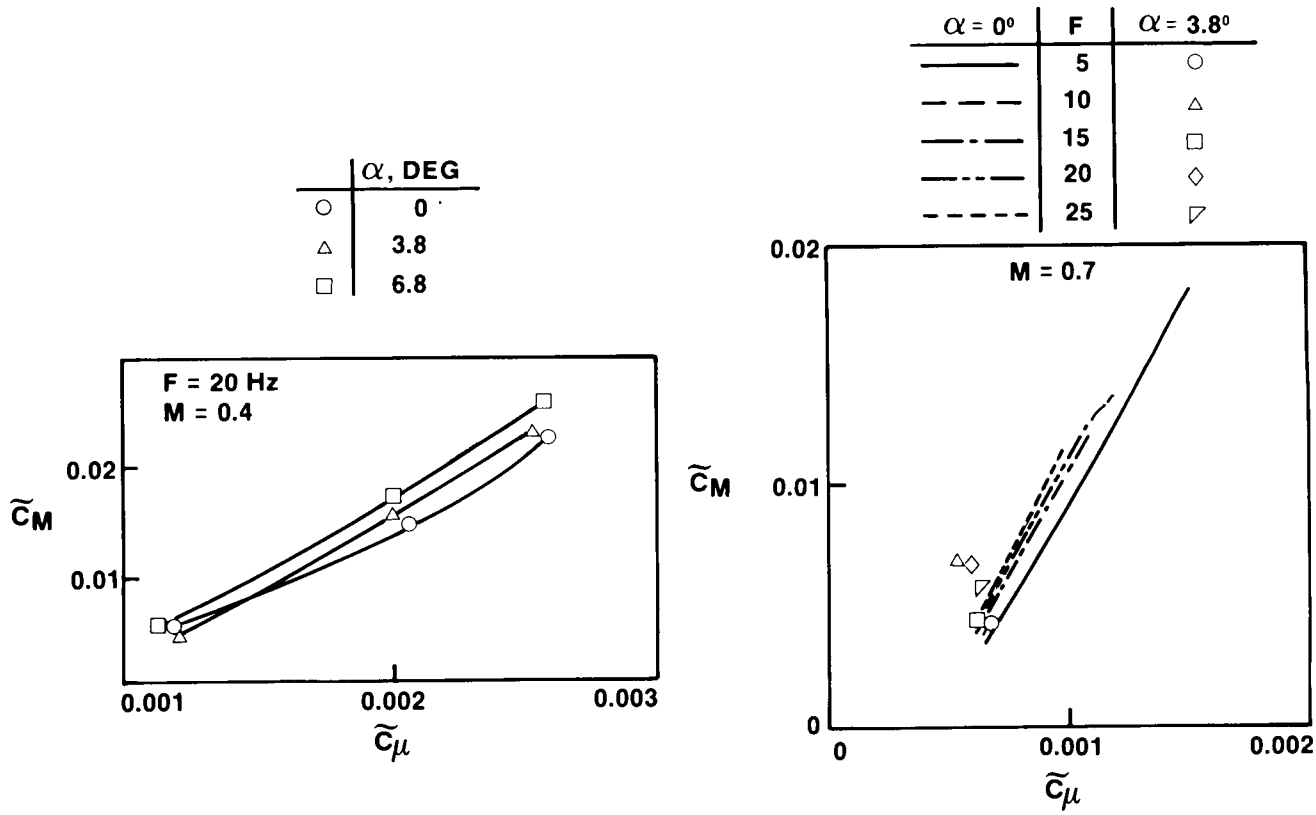

Figure 34. Fundamental Amplitude vs. Jet Momentum

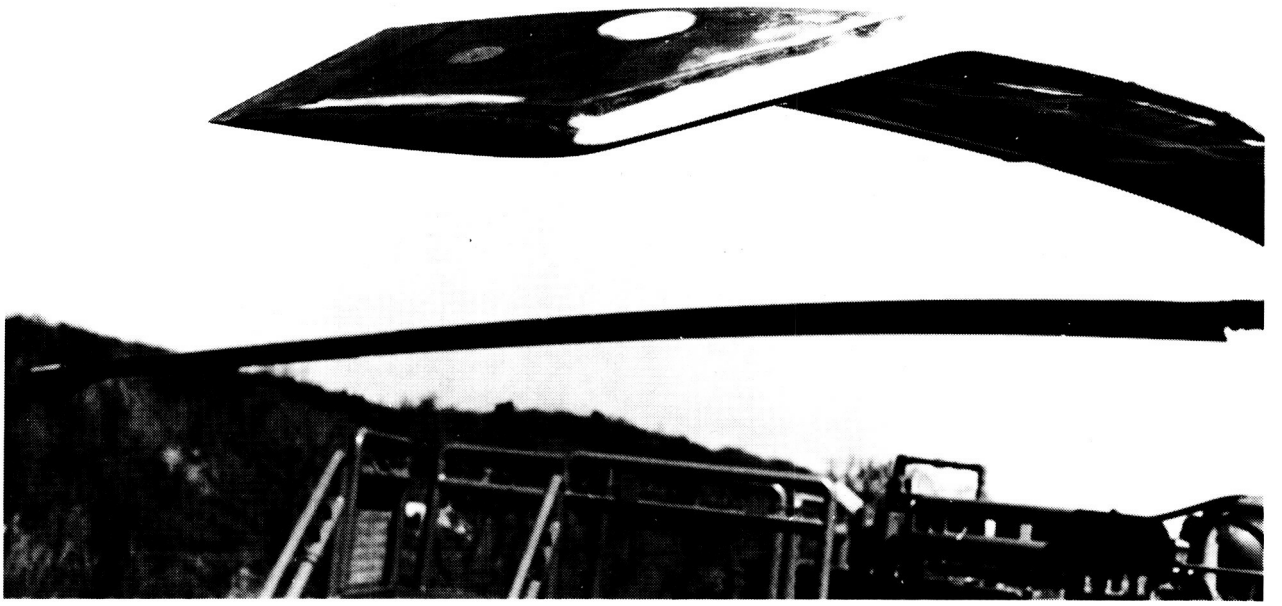

Figure 35. UH-60A Main Blade with Anhedral Tip Installed

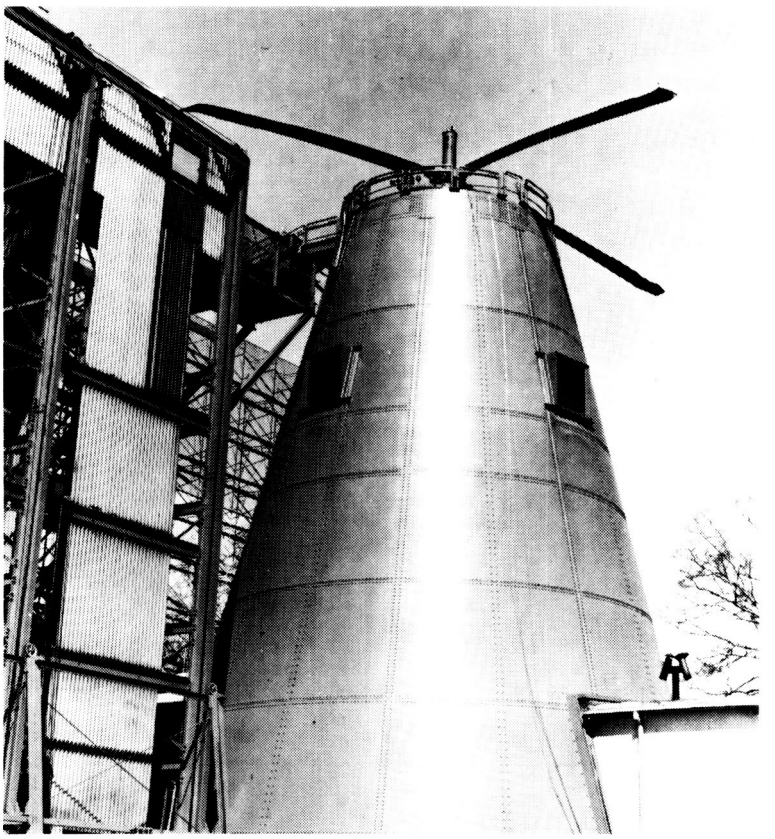

Figure 36. 10,000 Horsepower Main Rotor Stand with UH-60A Rotor System Installed with Anhedral Tip Caps

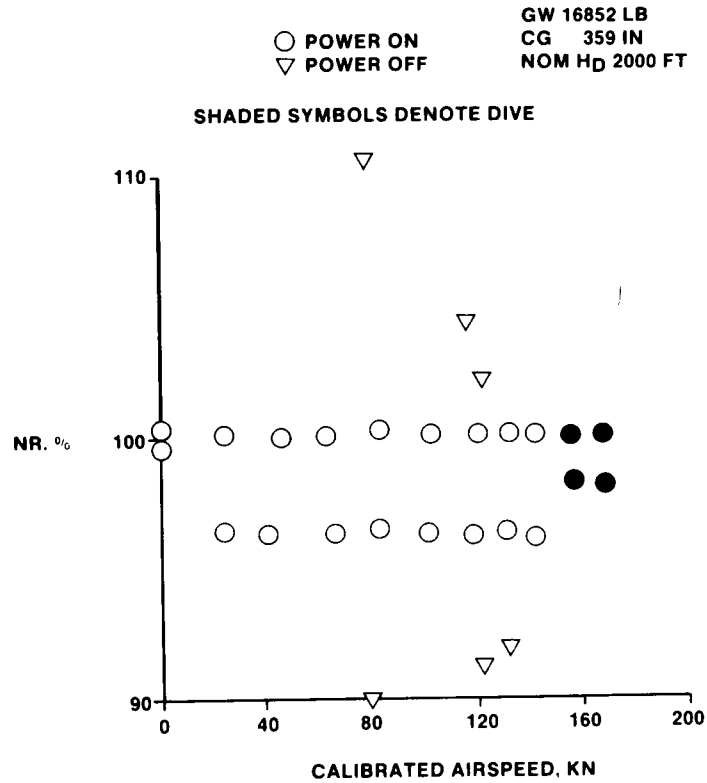

Figure 37. Main Rotor Speed Envelope for UH-60A Rotor with Anhedral Tip Caps

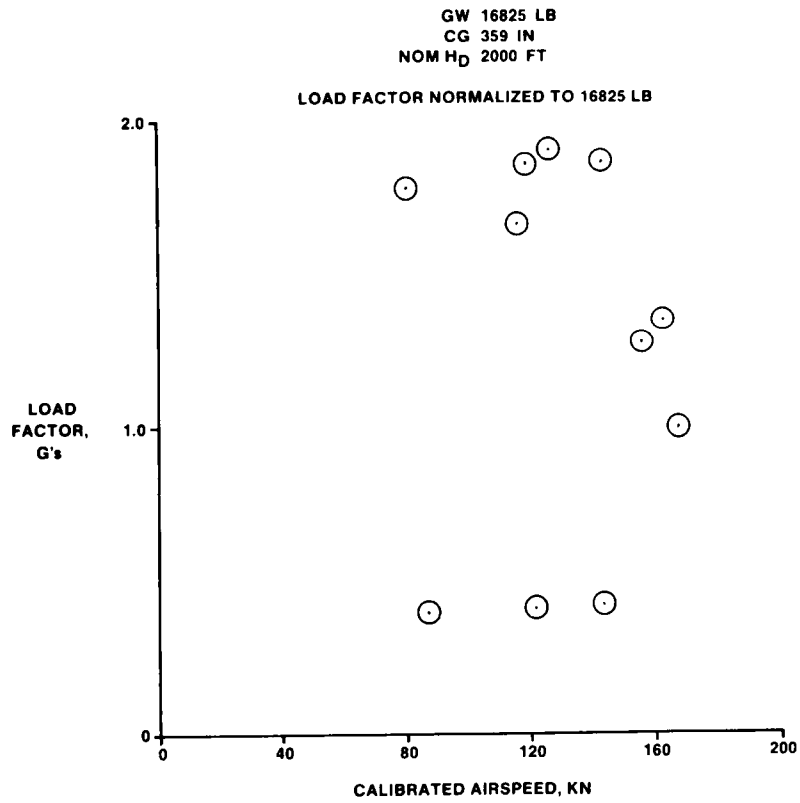

Figure 38. Load Factor Envelope for UH-60A Rotor with Anhedral Tip Caps

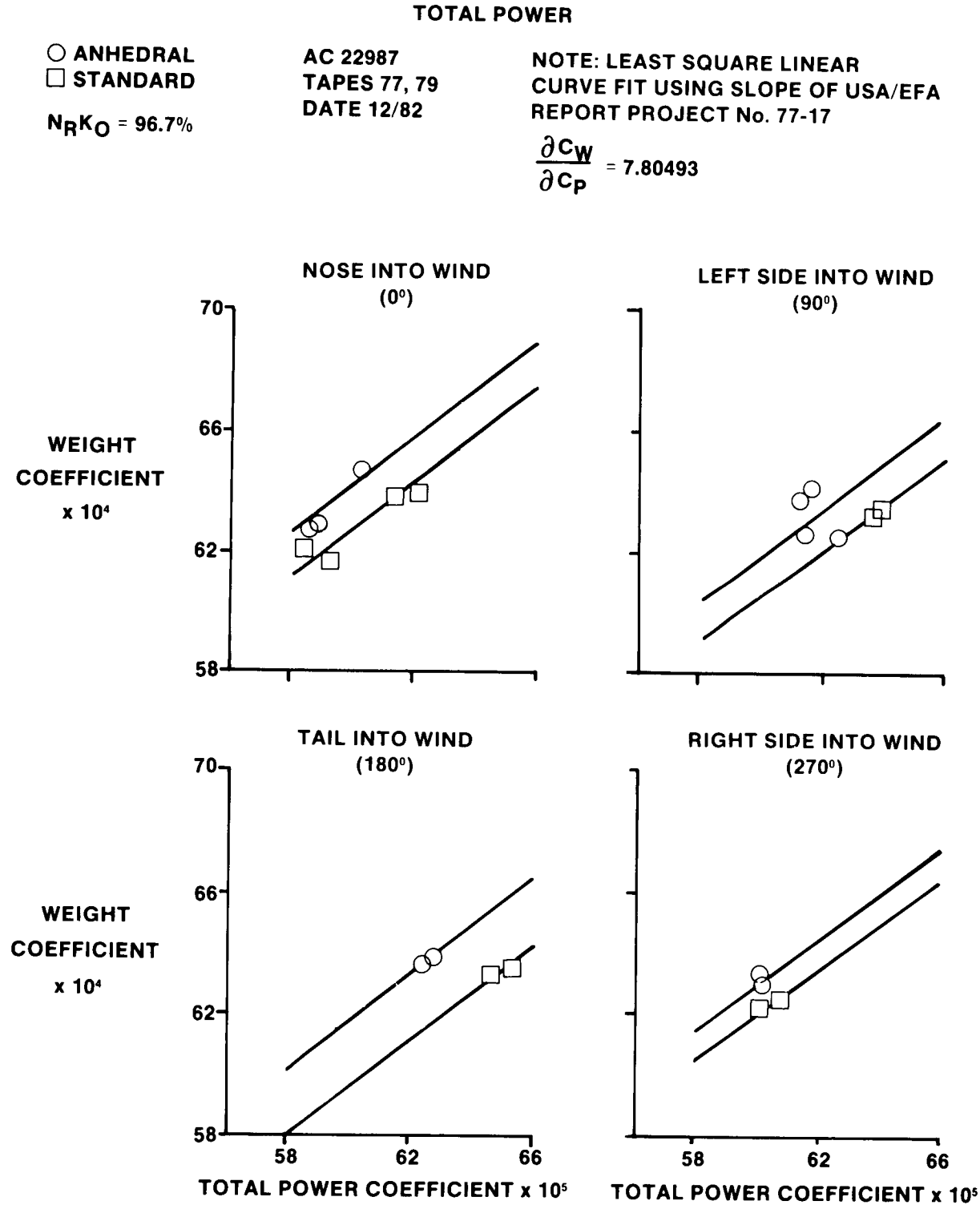

Figure 39. Nondimensional Hover Total Power vs. Wind Azimuth

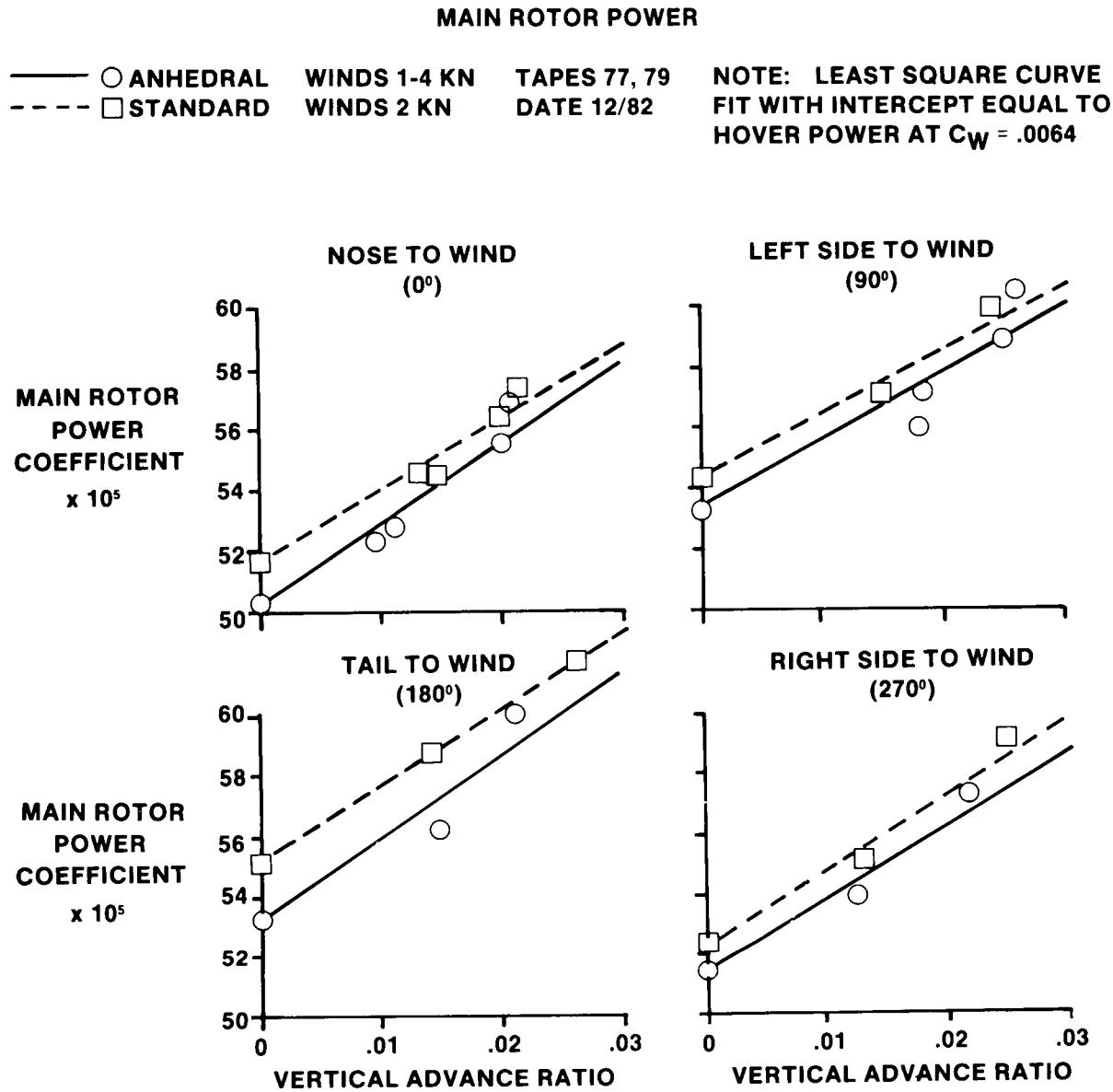

Figure 40. Nondimensinal Level Flight Power Required

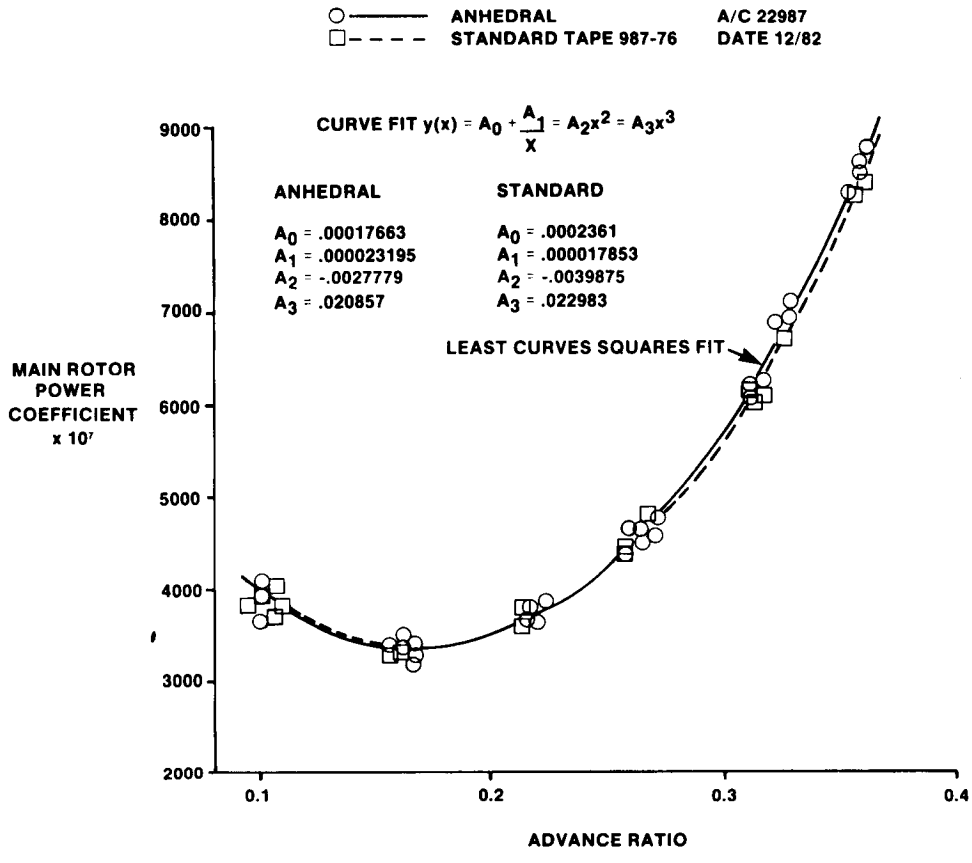

Figure 41. Nondimensional Level Flight Power Required

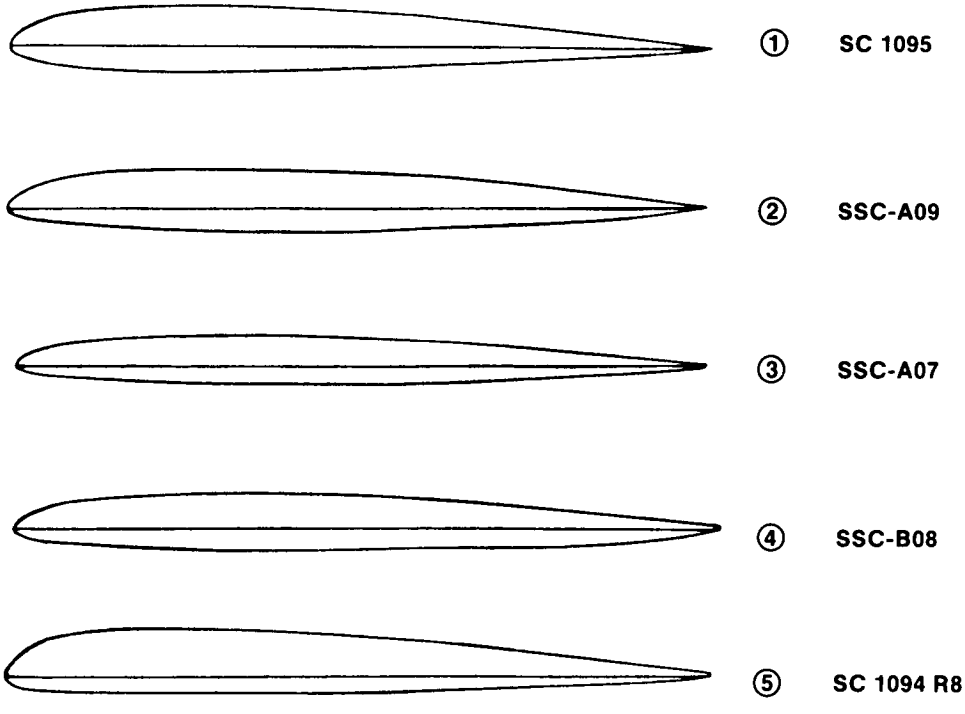

Figure 42. Airfoil Section Profiles

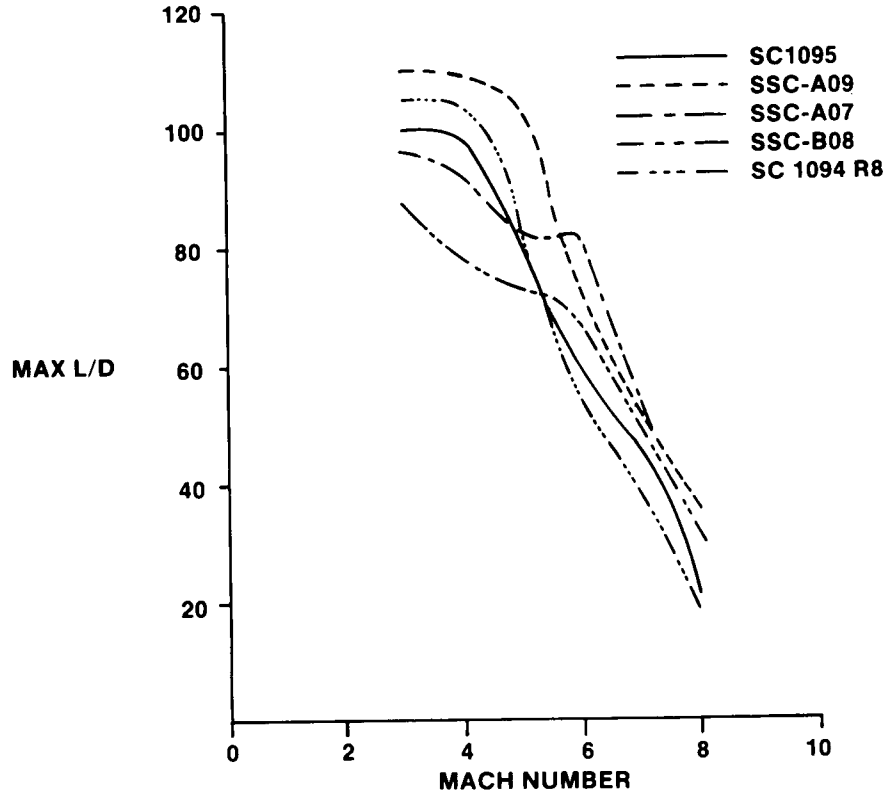

Figure 43. Maximum L/D vs. Mach Number

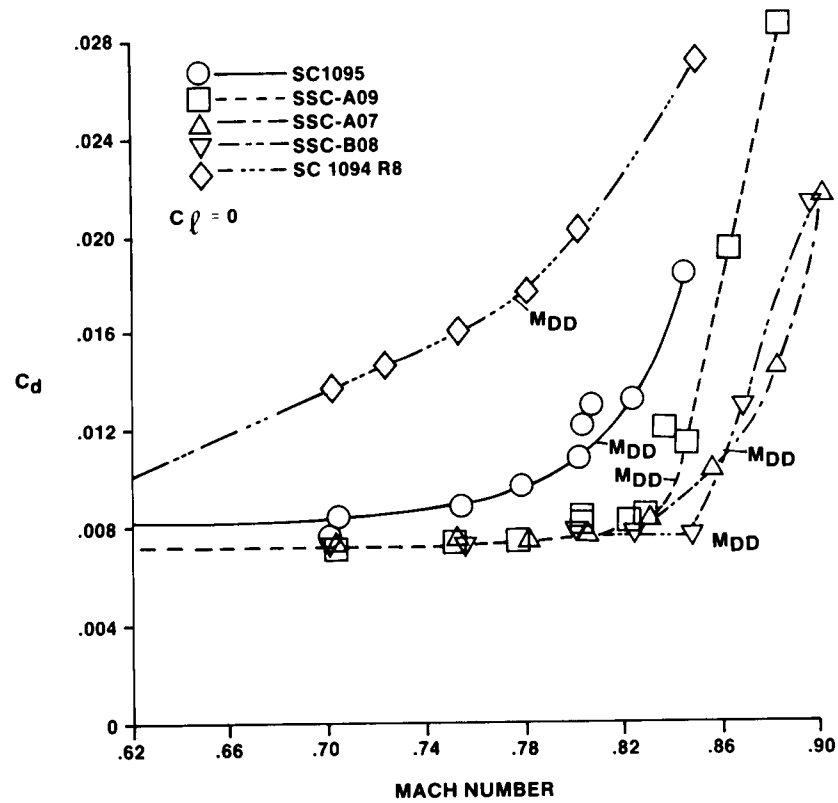

Figure 44. Variation in Drag Coefficient at Zero Lift vs. Mach Number

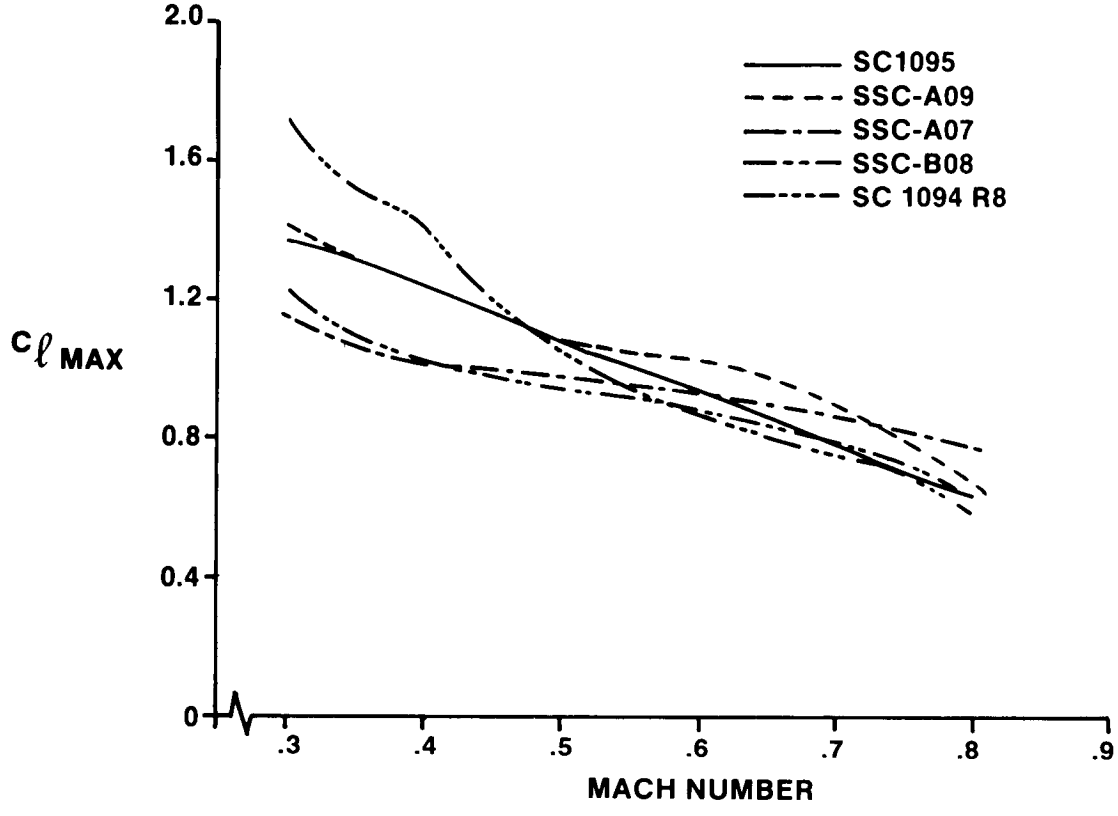

Figure 45. Variation in Maximum Lift Coefficient vs. Mach Number

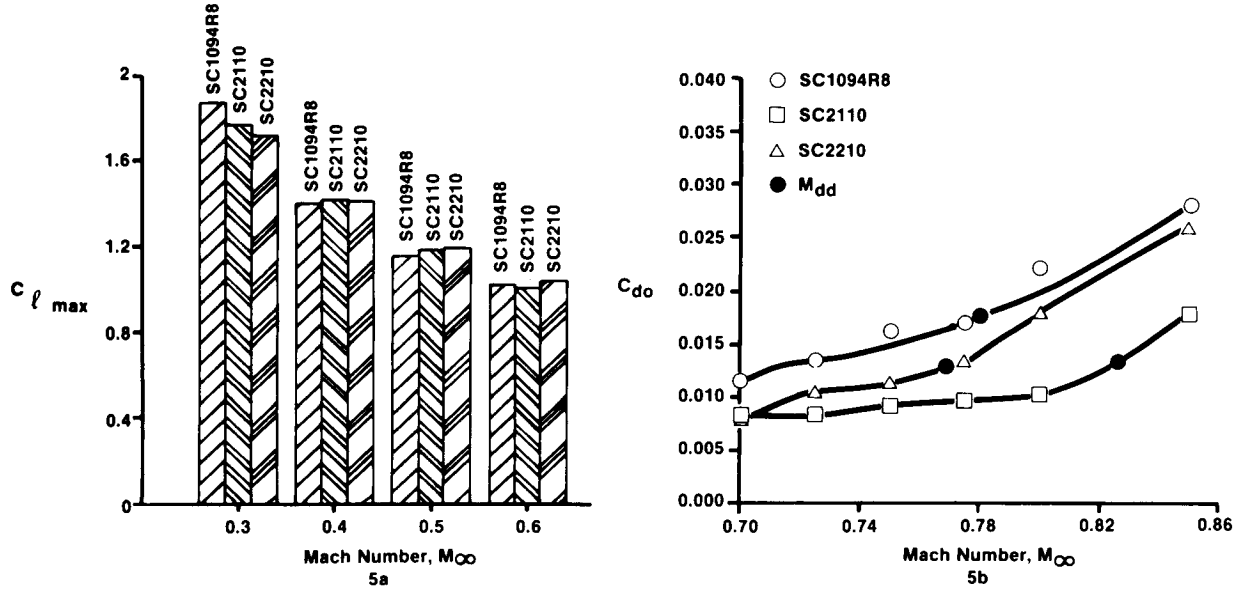

Figure 46. OSU Experimental Results for Maximum Lift and Zero Lift Drag, Baseline and Comparison Airfoils

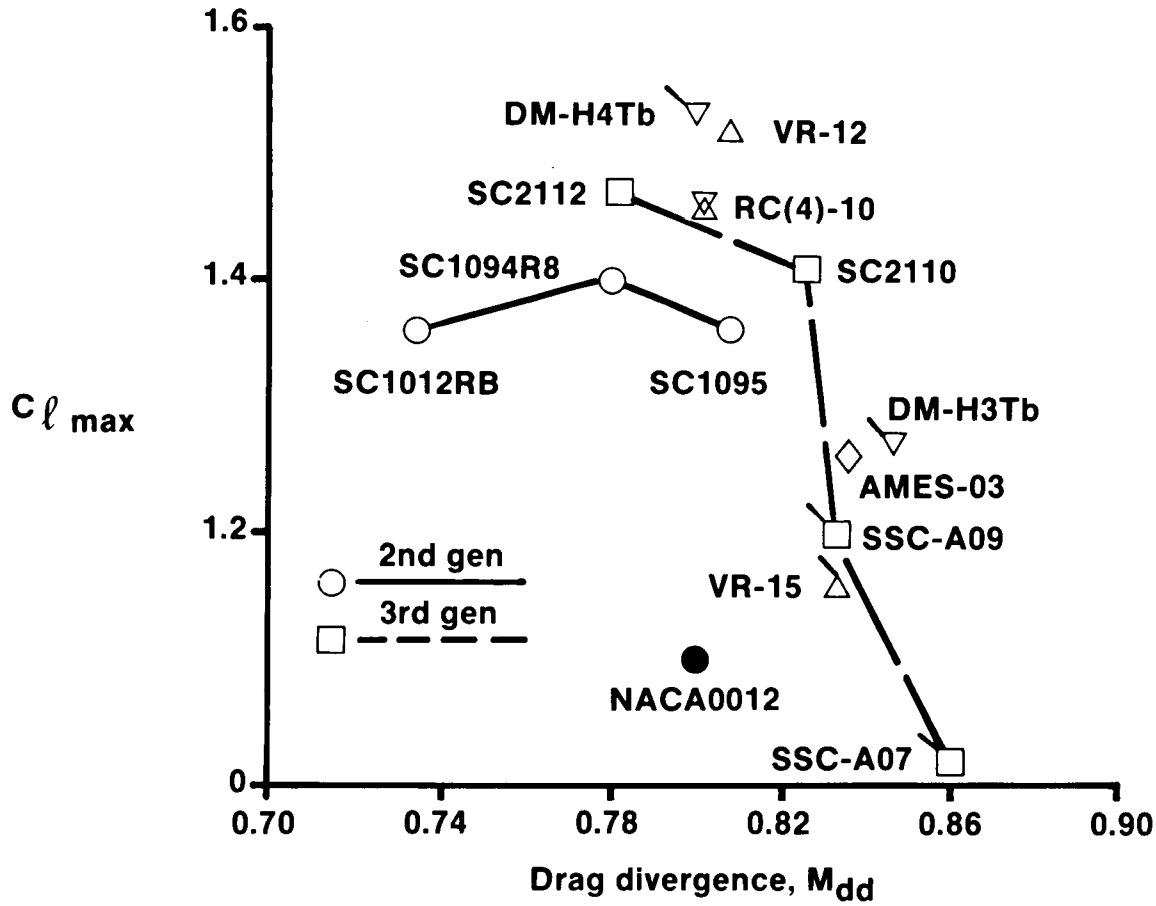

Figure 47. Third Generation Performance Improvements